HOW DOES CD8 LOSS IMPACT THE IMMUNE RESPONSE TO SYSTEMIC *SALMONELLA* INFECTION ?

BY SIÂN ELIZABETH FAUSTINI

A thesis submitted to the

University of Birmingham

For the degree of

MASTER OF RESEARCH

UNIVERSITY OF BIRMINGHAM

BBSRC
bioscience for the future

School of Immunity and Infection

College of Medical and Dental Sciences

University of Birmingham

October 2013

Abstract

Salmonella enterica serovar Typhimurium (STm) is an intracellular, gram-negative, facultative bacteria that causes two types of infection in humans: Typhoidal and Non-typhoidal *Salmonella* (NTS). NTS is known to cause a self-limiting gastroenteritis in the western world. However, it can be life-threatening to immunocompromised HIV-infected and non-infected individuals living in Sub-Saharan Africa. This study aimed to characterise the impact of CD8 loss in the immune response to STm in the spleen, peritoneal cavity, and thymus though the use of a knock out mouse strain (CD8 KO) and the infection with an attenuated STm bacterial strain (SL3261). Predominantly, $CD4^+$T-cells or Th1 cells are more important in producing IFN-γ and mediating bacterial clearance during primary infection. In contrast, the role of CD8 molecules during primary and secondary STm infection is less clear. Bacterial culture revealed that bacterial clearance is hindered at day 35 post-infection in CD8 KO mice. We observed a defect in the early extrafollicular (EF) response with regards to the production of lower levels of OMP-specific IgG at day 7 post-infection. This also inhibited isotype class-switching; thus, IgG2b and IgG2a (IgG2c in C57BL/6 mice) antibody levels were also low. Thus, the absence of CD8 molecules must impact the early T_{FH} response during thymus-dependent (TD) antibody responses. In future experiments, it would be useful to characterise the immune response to STm in CD8 KO mice using a virulent strain of STm, SL1344 to see if primary infection with the attenuated strain allows for the conferred protection once challenged with the virulent strain.

Table of Contents

Abbreviations

AP	Alkaline phosphatase
APC	Antigen Presenting Cell
Bt	Biotin
CD4	Cluster of Differentiation-4
CD8	Cluster of Differentiation-8
CFU	Colony Forming Units
DAB	3,3´-diaminbenzidine tetrahydrochloride
DC	Dendritic Cell
DN	Double Negative
EDTA	Ethylenediaminetetraacetic acid solution
EF	Extrafollicular Response
ELISA	Enzyme-Linked Immunosorbent Assay
ELISpot	Enzyme-Linked Immunosorbent Spot Assay
FACS	Fluorescent Activated Cell Sorting
FAE	Follicle Associated Epithelium
FCS	Foetal Calf Serum
HRP	Horse Radish Peroxidase
Ig	Immunoglobulin
I.P.	Intraperitoneal
IFN-γ	Interferon-gamma
IHC	Immunohistochemistry
IL	Interleukin
KO	Knock out
LB	Luria Bertani
LPS	Lipopolysaccharide
MHC	Major Histocompatibility Complex

MLN	Mesenteric Lymph Node
MZ	Marginal Zone
NKT	Natural Killer T-Cells
NOS	Nitric Oxide Synthase
NTS	Non-Typhoidal *Salmonella*
OD	Optical density
OMPs	Outer Membrane Proteins
PBS	Phosphate Buffered Solution
pDCs	Plasmacytoid Dendritic Cells
PEC	Peritoneal Cavity
pNPP	p-Nitrophenylphosphate
Px	Peroxidase
RBCs	Red Blood Cells
RP	Red pulp
SCV	*Salmonella*-containing vacuole
SP	Single Positive
SP1-1	*Salmonella* Pathogenicity Island-1
SP2	*Salmonella* Pathogenicity Island-2
STm	*Salmonella enterica* serovar Typhimurium
TCR	T-cell receptor
TD	Thymus-dependent
T_{FH}	T-follicular helper cell
Th1	T helper 1 cell
TI	Thymus-independent
TNF-α	Tumour Necrosis Factor- alpha
WP	White pulp
WT	Wild-type

Chapter 1: Introduction

1.1 *Salmonella enterica* serovar Typhimurium

Salmonella enterica serovar Typhimurium (STm) is an intracellular, gram-negative, facultative bacteria that causes two types of infection in humans: Typhoidal and Non-typhoidal salmonella (NTS).

1.1.1 Non-typhoidal *Salmonella* (NTS)

NTS is characterised by its self-limiting gastroenteritis in the western world. However, in Sub-Saharan Africa, NTS can be lethal to immunocompromised, HIV-infected individuals, including children who are not infected with HIV (Dougan et al., 2011).

NTS causes a systemic, typhoid-like disease that involves the initial infection of intestinal Peyer's patches and rapid dispersal to the blood, bone marrow, liver, spleen, and thymus (Moon and McSorley, 2009). Membranous (M) cells, which reside in the follicle-associated epithelium (FAE) just above the Peyer's patches, and dendritic cells (DCs), professional antigen presenting cells (APCs), induce the uptake of STm in the intestine and deliver them to resident macrophages below the FAE (Hughes and Galan, 2002).

1.1.2 STm Pathogenesis

STm is a very robust bacterium. It can survive within APCs and replicate within phagocytes of the bone marrow, liver, spleen, and thymus. Furthermore, STm replicates within a modified endosome also known as the *Salmonella*-containing vacuole (SCV). Thus, STm manipulates the intracellular environment of the phagocyte through the

encouragement of optimal growth conditions via protein activity induced by the type III secretion system encoded by Salmonella pathogenicity island-2 (SP2) (Jackson et al., 2010, Gog et al., 2012, Hensel, 2000, Santos et al., 2001, Griffin and McSorley, 2011, Mittrucker and Kaufmann, 2000). Furthermore, STm persist within phagocytes via the inhibition of phago-lysosomal fusion and acidification within the SCV (Dougan et al., 2011). Typically, the environment of the phagocyte is characterised by poor nutrient availability, low pH, and constant exposure to antimicrobial peptides and enzymes (Luu et al., 2006). STm will rapidly infect and divide within the intracellular compartments of the vast population of macrophages (Jackson et al., 2010). Thus, STm can quickly overwhelm the host through the evasion of immune surveillance and bactericidal killing (Jackson et al., 2010).

1.1.3 Animal Model of *Salmonella* infection

The murine model of STm infection has been well-studied and is extensively used for the investigation of typhoid fever. Furthermore, the STm model of infection has similarities to human typhoidal infection caused by *Salmonella enterica* serovar Typhi (Moon and McSorley, 2009, Mittrucker et al., 2002).

After a few days of initial infection, STm rapidly colonises the liver, spleen, and thymus and high bacterial loads persist until the host can limit bacterial growth. This period will normally last for a few-weeks until the host's adaptive immune system sequesters bacterial replication and establishes a defence against reinfection (Mittrucker et al., 2002). Thus, $CD4^+$T-cell and $CD8^+$T-cell activation and the production of antibodies orchestrate an effective adaptive immune response that reduces and clears bacterial

infection within the host (Gil-Cruz et al., 2009, Cunningham et al., 2007, Mittrucker and Kaufmann, 2000, Mastroeni and Sheppard, 2004).

Splenomegaly, an enlargement of the spleen, is a common hallmark of STm infection. It is initiated in the spleen and not from the peripheral circulation (Jackson et al., 2010, Mittrucker et al., 2002, Griffin and McSorley, 2011). Additionally, it occurs due to the vast recruitment and expansion of many activated cells such as T- and B- lymphocytes and phagocytes to the spleen (Mittrucker et al., 2002, Jackson et al., 2010). Splenic weight size is directly proportional to bacterial burden. Thus, cellular recruitment and migration causes major disruptions to the splenic architecture and T-and B- cell zones lack definite structure. Thus, these factors collectively contribute to the ten-fold increases in splenic size (Cunningham et al., 2007, Jackson et al., 2010, Mittrucker et al., 2002).

In vivo models of STm infection, in particular with SL3261, an attenuated strain of STm, allows for the investigation of induction and resolution of bacterial infection, as well as the evaluation of bacterial and host interactions. Furthermore, genetic manipulations can be employed to the host (i.e. knockout mice (KO)) in order to assess requirements for innate and adaptive immune responses during the course of STm infection (Mastroeni et al., 2009, Santos et al., 2001). The bacterial burden of 10^8 STm within tissue is considered to be the approximate threshold for mouse survival. Furthermore, as bacterial titres exceed this threshold, infected mice will succumb to bacteremia, endotoxic shock, and death (Mittrucker and Kaufmann, 2000). Typically, infection is established with 5×10^5 attenuated SL3261 in the Cunningham laboratory model of STm infection.

1.2 The Host and the Immune System

1.2.1 Innate Immunity to STm

Rapid dissemination of STm bacteria triggers the innate immune system to respond to the initial infection in order to monitor and reduce bacterial replication until the adaptive immune system mounts a response. Thus, innate immunity to STm requires complement mediated killing pathways in order to keep infection from overwhelming the host (MacLennan et al., 2008). Additionally, DCs, macrophages, neutrophils, and natural killer (NK) T-cells produce IFN-γ during the first few weeks of STm infection in order to limit bacterial growth (Jackson et al., 2010). STm bacterial growth is limited by macrophage migration inhibitory factor and Nramp1 (mice only), an innate resistance autosomal dominant gene, which resides on chromosome 1 and is expressed predominantly in macrophages (Mastroeni and Sheppard, 2004, Dougan et al., 2011).

STm-infected macrophages can induce the production of reactive nitrogen and oxygen intermediates, as well as lysosomal enzymes that can severely pre-empt bacterial replication within the host (Griffin and McSorley, 2011).

Initially, the innate immune response is established and chemokines recruit monophils and neutrophils to the site of STm colonisation where they induce nitric oxide (NO) synthase in order to kill STm bacteria (Jackson et al., 2010, Dougan et al., 2011).

STm cell wall components of including lipopolysaccharide (LPS) and flagellin are known to induce an innate immune response via the production of Th1 (T-helper 1) cytokines such as IFN-γ, TNF-α (Tumour Necrosis Factor-α), IL-6 (Interleukin 6) , IL-8, IL-12, and IL-18 (Dougan et al., 2011).

Although the innate immune response is effective at limiting bacterial replication in the host for the initial stages of STm infection, it does not completely eradicate STm from the immune system. Thus, the acquired immune response is needed to achieve sterile immunity in the host.

1.2.2 Adaptive Immunity to STm

1.2.2.1 Cell-mediated immunity

STm rapidly infects and divides within host macrophages, yet triggers the production of IFN-γ by Th1 (T-helper 1) cells which inhibits bacterial growth (Moon and McSorley, 2009, Jackson et al., 2010, Gog et al., 2012).

1.2.2.1.1 $CD4^+$T-cells

Th1 or $CD4^+$T-cells play an extremely important role in cell-mediated immunity. Additionally, T_{FH}, T-follicular helper, cells are a particular subset of $CD4^+$T-cells that are involved in driving T-cell responses and antigen-specific B-cell immunity i.e. the generation of memory B-cells and plasma cells. T_{FH} cells express Bcl6, a master regulator transcription factor (Crotty, 2011). Bcl-6 expression is necessary for B-cell class switching (Lee et al., 2011). Furthermore, T_{FH} cells help to form and maintain germinal centres (GCs), including the regulation of B-cell differentiation into memory B-cells and plasma cells (Crotty, 2011). T_{FH} cells express cytokines such as IFN-γ and IL-17 that control isotype class-switching (Crotty, 2011). Th1 and T_{FH} cells play a key role in the immune response to STm and their differentiation pathways are depicted in Figure 1.1.

Antigenic peptides presented by DCs activate naïve $CD4^+$T-cells via a TCR (T-cell receptor) in the MHC-Class II pathway (Moon and McSorley, 2009). Once activated, these effector $CD4^+$T-cells produce IFN-γ and TNF-α in response to MHC Class II recognition of

STm-infected phagocytes and presentation of antigenic peptides. Th1 cells are detected as early as one week into the infectious period and comprise more than 50% of all CD4⁺T-cells in circulation as early as two to three weeks into infection (Griffin and McSorley, 2011)

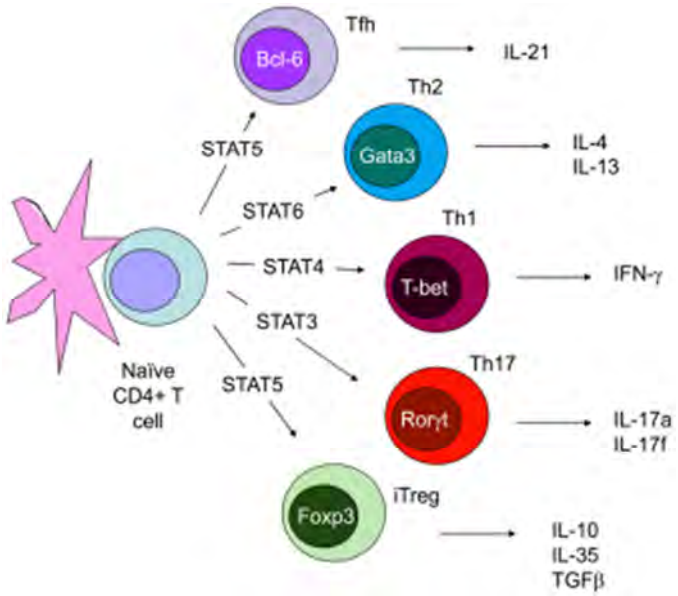

FIGURE 1.1. A CLASSICAL VIEW OF HELPER CD4⁺T-CELL DIFFERENTIATION. PICTURE SHOWS A DC PRIMING A NAÏVE CD4 ⁺T-CELL, EFFECTOR SUBSETS, AS WELL AS CYTOKINE SECRETION. *PICTURE TAKEN FROM (O'SHEA AND PAUL, 2010).*

1.2.2.1.2 CD8⁺T-cells

STm also triggers the activation and dissemination of CD8⁺T-cells (Jackson et al., 2010). However, the role of CD8⁺T-cells in STm infection is poorly characterised and less understood (Moon and McSorley, 2009).

Furthermore, there have been conflicting studies using a virulent strain of STm (SL1344) that have suggested that CD8⁺T-cells are important for clearing bacterial infection in primary infection (Luu et al., 2006, Lo et al., 1999, van der Velden et al., 2005), whilst other studies using an attenuated strain of STm (SL3261) have suggested

only a minor role for reducing bacterial numbers in primary infection (Lee et al., 2012, Hess et al., 1996, Mastroeni et al., 1992).

More interestingly, infection with ST-YopE-Ova (recombinant STm that incorporates ovalbumin (OVA) into a plasmid that codes for a Yersinia outer-membrane protein E (YopE)) suggests that once $CD8^+$T-cells are made to recognise STm antigens, they are considered extremely important in mediating immune surveillance in primary infection (Tzelepis et al., 2012). Furthermore , adoptive transfer experiments have shown that $CD8^+$T-cells play a role in the acquired immunity to STm infection (Nauciel, 1990).

1.2.2.2 Humoral immunity

Antibody (Ab) or humoral immunity is required for protective immunity against secondary infection (Moon and McSorley, 2009). B-cells and subsequently, the production of antibodies, are not required for the resolution of primary STm infection; however, they are required for an acquired immune response once challenged at a later time (Griffin and McSorley, 2011). Antibody can have direct access to STm in the extracellular compartment once infected phagocytes have undergone apoptosis. Thus, the antibody opsonizes the extracellular STm and prevents it from infecting an adjacent phagocyte (Cunningham et al., 2007, Griffin and McSorley, 2011).

1.2.3 Sites of STm colonisation

1.2.3.1 The Spleen

The spleen is a secondary lymphoid organ that is located in the abdominal cavity and connected to the stomach (Mebius and Kraal, 2005). It collects antigens from the blood, as well as the collection and disposal of old erythrocytes (Janeway et al., 2005). The

spleen is composed of red pulp and white pulp, which is divided by the marginal sinus (Figure 1.1)(Vale and Schroeder, 2010).

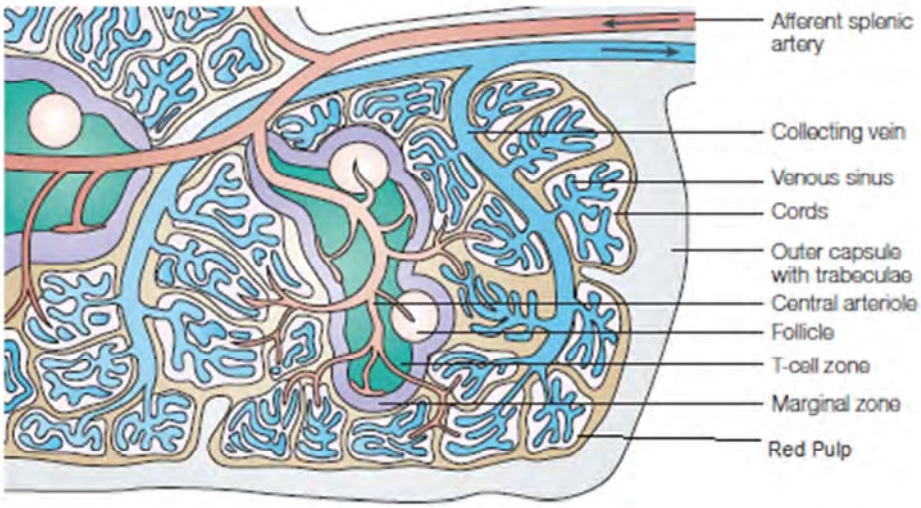

Figure 1.2. Structure of the spleen, which includes the clearly defined regions of red pulp, white pulp, MZ, T-cell zones, as well as B-cell follicles. *Adapted from Mebius and Kraal (2005).*

1.2.3.1.1 Red Pulp

The red pulp is the main location for erythrocyte disposal (Janeway et al., 2005). Macrophages, a type of APC, are found within the red pulp and are intrinsic in the removal of bacteria from the blood. Signalling cascades via toll-like receptors (TLRs) begin once macrophages have encountered bacteria and they secrete molecules that inhibit the growth of bacteria (Mebius and Kraal, 2005). Plasmablasts and plasma cells are also located within the red pulp. Plasmablasts are activated B-cells that have not differentiated into mature plasma cells (Mebius and Kraal, 2005). Initially, they

differentiate in the follicles of the white pulp and then migrate to the red pulp. After subsequent migration to the red pulp, they migrate through the lymph and blood to travel to sites where they will mature into antibody-producing plasma cell factories (Mebius and Kraal, 2005)

1.2.3.1.2 White Pulp

The white pulp regions are composed of lymphocytes that surround the arterioles of the spleen (Janeway et al., 2005). Furthermore, these areas contain clearly defined B-cell follicles and a T-cell zone (Mebius and Kraal, 2005).

1.2.3.1.2.1 B-Cell Follicles

B-cells form follicles, which are sites of clonal expansion for activated B-cells (Mebius and Kraal, 2005). T-cells, previously primed by DCs in the T-zone, subsequently prime B-cells within the T-zone (Section 1.2.3.1.2.2). Activated follicular B-cells will go on to proliferate and form GCs or differentiate into plasmablasts. They can also differentiate into non-proliferating plasma cells, which also secrete antibody (MacLennan et al., 2003) . These events are part of the extrafollicular response (EF) (Figure 1.3) , which is responsible for the rapid generation of antibodies following a pathogen encounter (MacLennan et al., 2003). An EF response can also trigger antibody class-switching and somatic hypermutation, which is defined as introducing variation into the variable region of immunoglobulin for positive and negative selection of antigen-binding sites (Janeway et. al, 2005).

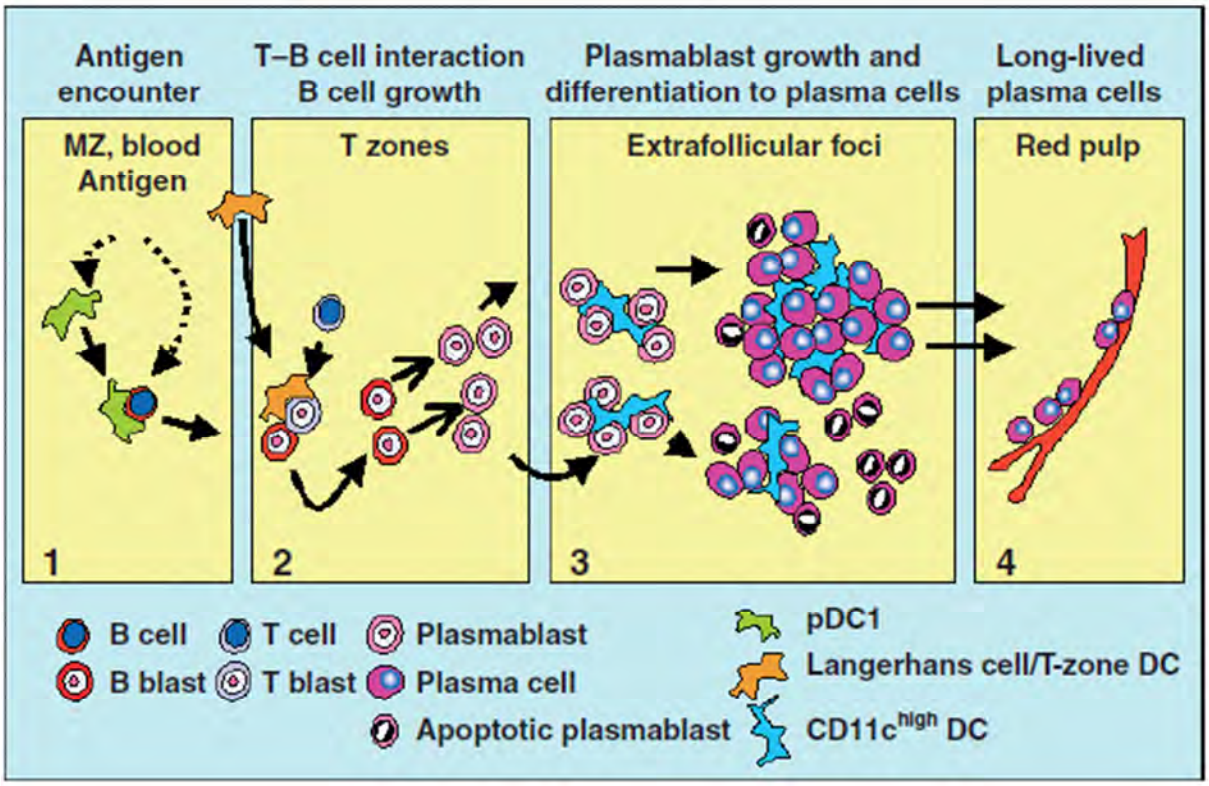

Figure 1.3. The Extrafollicular Antibody Response (EF). *Picture taken from MacLennan et al. (2003).*

1.2.3.1.2.2 T-Cell Zone

T-cell zones consist of T-cells that display interactions with B-cells and DCs (Mebius and Kraal, 2005). Once APCs enter the white pulp, activated T-cells migrate to B-cell follicles and activate B-cells. Once activated, B-cells will class-switch and then migrate to the GCs, MZ, or red pulp (Mebius and Kraal, 2005). This is an example of T-dependent activation of B-cells.

1.2.3.1.2.3 Marginal Zone

The marginal zone (MZ) is another important cell-transit region that surrounds the white pulp (Mebius and Kraal, 2005). It is characterised as a highly organized region composed of a large population of macrophages and a select population of B-cells, also

known as MZ B-cells and a small population of follicular dendritic cells (FDCs) (Janeway et al., 2005). The macrophages trap blood-borne pathogens in the MZ (Janeway et al., 2005). The MZ B-cells act quickly to inhibit pathogen invasion by acting as APCs or differentiating into plasma cells that produce IgM (Mebius and Kraal, 2005). MZ B-cells express the phenotype of IgMhi, CD1dhi, CD9hi, CD21hi, CD22hi, IgDlo,CD23lo, and B220lo. Activated MZ B-cells can act as APCs by obtaining antigenic peptides within the MZ and migrating into the white pulp where they can activate naïve $CD4^{+}$T-cells (Mebius and Kraal, 2005). FDCs may possess long processes like DCs; however, they are distinctly different from other types of DCs because they are not phagocytic and do not derive from bone marrow precursors (Janeway et al., 2005). Furthermore, FDCs do not express MHC-Class II on their cell surfaces (Janeway et al., 2005). FDCs are derived from mesenchymal stem cells and display receptors for complement and F_c (Banchereau and Steinman, 1998). FDCs are entirely distinct from other types of DCs because they do not process the antigen (Vale and Schroeder, 2010). Instead, FDCs are responsible for presenting antigen in the form of immune complexes to activate B-cells within the B-cell follicle (Vale and Schroeder, 2010). In turn, these follicular B-cells become activated and differentiate and play a major role in the adaptive immune response (Vale and Schroeder, 2010).

1.2.3.1.2.3.1 T-independent response

B-cells can respond via direct contact with an antigen in contrast to T-cells, which require an APC to become activated (Vale and Schroeder, 2010). Once a B-cell is activated, it can divide and differentiate into memory cells or activated plasma cells that become antibody factories.

1.2.3.1.2.3.2 T-dependent response

MHC Class I and II molecules are both present on activated B-cells. Thus, B-cells can engulf and present an antigenic peptide to $CD4^+$T-cells and $CD8^+$T-cells (Vale and Schroeder, 2010). B and T-cells can actively co-stimulate each other once they bind the same antigenic peptide, which enhances the adaptive immune response if challenged with the same pathogen in the future (Vale and Schroeder, 2010).

GCs also play a large role in the humoral or B-cell mediated response to an infection. GCs form in the white pulp as a result of the interaction and subsequent activation between T-cells and B-cells within the first 3 weeks of antigenic exposure (Vale and Schroeder, 2010, MacLennan, 1994). Additionally, affinity maturation, somatic hypermutation, and antibody class switching occur within a GC (MacLennan, 1994). Affinity maturation is defined as the selection and subsequent survival of B-cells with high affinity for a particular antigen (Janeway et al., 2005). Antibody or isotype class switching is the selection of B-cells to differentiate into effector cells that promote the secretion of antibodies with different isotypes (Janeway et al., 2005).

1.2.3.2 The Peritoneal Cavity

The peritoneal cavity provides a niche for B1b cells, which are self-renewing and have unique activation properties and cell cycles that differ markedly from B2 cells that reside in the spleen and lymph nodes (Martin and Kearney, 2002). Furthermore, PEC (peritoneal cavity) cells are known to share some properties to MZ B-cells (Martin and Kearney, 2002). Additionally, B1b cells are precursors to cells that secrete IgM (Martin and Kearney, 2002). B1a and B1b cells express the surface marker phenotype IgM^+,

IgD^{low}CD21^{low}CD23^{low}B220^{int}CD19^{+} and CD11b variable (Marshall et al., 2012). B1b cells are intrinsic for mounting a protective antibody response to pathogens (Marshall et al., 2012).

1.2.3.3 The Thymus

The thymus, located in the upper anterior thorax, is composed of two lobes, which each consist of an outer cortical region and an inner medulla (Janeway et al., 2005). The thymus is the site for differentiation of T-cells (Nunes-Alves et al., 2013). T-cell differentiation (Fig. 1.4) depends on the type of antigen that thymocytes encounter, as well as the surrounding thymic architecture and environment (Nunes-Alves et al., 2013).

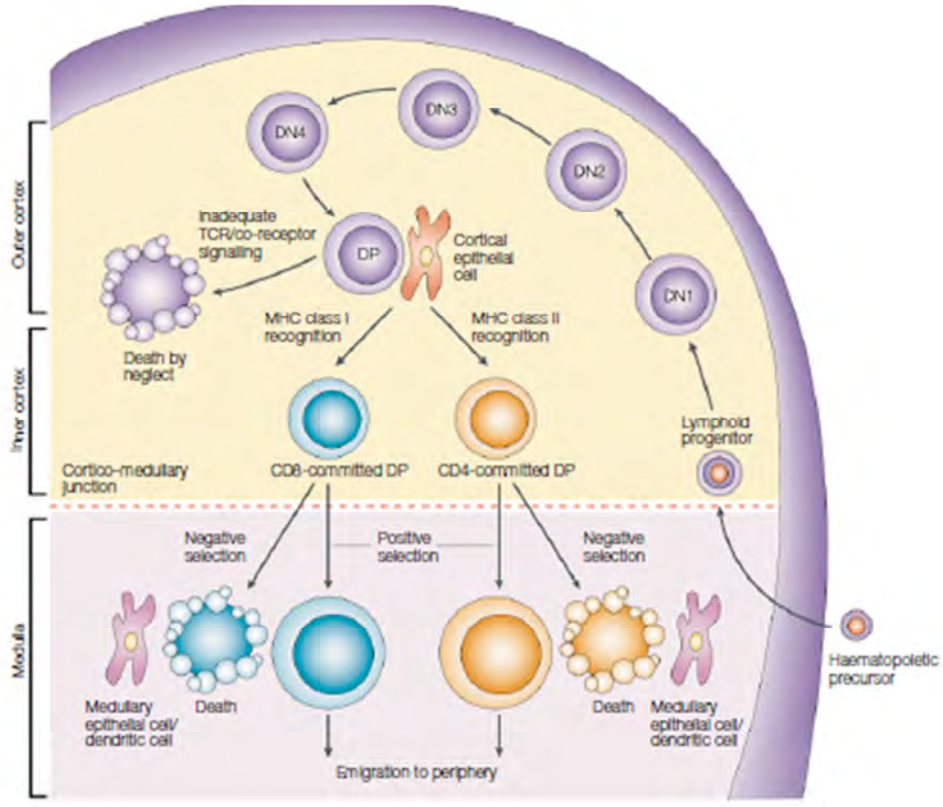

Figure 1.4. T-cell differentiation and positive and negative selection in the thymus. *Image taken from Germain (2002).*

1.2.3.3.1 Thymic Cortex

The thymic cortex consists of an outer region that is comprised of proliferating immature thymocytes and a deeper region that consists of immature T-cells undergoing positive or negative thymic selection (Fig. 1.4) , which pre-empts the proliferation of self-reactive T-cells (Nunes-Alves et al., 2013)(Janeway et al., 2005). Thymocytes are derived from double-negative (DN) CD4 and CD8 cells and mature to CD4 single-positive (SP) or CD8 single positive (SP) via CD4 and CD8 double positive intermediates (Ross et al., 2012). Positive selection is defined as the maturation of immature thymocytes into $CD4^{+}$T-cells and $CD8^{+}$T-cells induced by T-cell receptor (TCR) signals that result from binding to MHC Class II or I ligands, respectively (Germain, 2002). Negative selection is defined as thymocyte cell loss via apoptosis within the thymus due to an overwhelming T-cell signalling response(Germain, 2002). Additionally, the cortex consists of branched cortical epithelial cells and dispersed macrophages (Janeway et al., 2005).

1.2.3.3.2 Thymic Medulla

The inner medulla is comprised of medullary epithelial cells, mature thymocytes, macrophages, and dendritic cells (Janeway et al., 2005). T-lymphocytes or T-cells derive from a common lymphoid progenitor in the bone marrow that migrate and commit to development within the thymus (Janeway et al, 2005).

1.2.3.3.3 Thymic atrophy is induced as a result of STm infection

Infection can affect the thymus locally and systemically (Nunes-Alves et al., 2013). Additionally, thymic atrophy occurs as a direct result of STm infection. It is characterised by a steady decrease in the number of thymocytes (Nunes-Alves et al., 2013). However, the reasons for thymic atrophy are less understood. One hypothesis is that thymic atrophy is a mechanism of pathogen virulence, which shields the pathogen from the

immune response. Another hypothesis is that atrophy is simply a by-product of infection which does not possess a significant advantage to either the pathogen or the host. The last hypothesis is that the host induces thymic atrophy in order to reduce thymic output during infection in order to pre-empt the disruption of T-cell selection and central tolerance to the invading pathogen (Nunes-Alves et al., 2013). On the contrary, it was found that although thymic atrophy accompanies STm infection, thymic output is not reduced and $CD4^+$T-cell export is maintained (Ross et al., 2012). Furthermore, it is important to note that the number of thymocytes recovers in the thymus as the STm infection clears the host and atrophy is resolved (Ross et al., 2012). This particular study suggests that thymic atrophy and thymic output are entirely exclusive from one another (Nunes-Alves et al., 2013, Ross et al., 2012).

1.3 CD8 Molecules in STm Infection

CD8 (Cluster of Differentiation 8) molecules, also known as CD8 receptors, interact with Major Histocompatibility (MHC) Class I complexes. These complexes are defined as a collection of genes that encode membrane glycoproteins that subsequently present antigenic peptides to T-cells (Janeway et al., 2005). The CD8 ligand binds to the MHC Class I molecule, which presents an antigenic peptide from an ingested intracellular pathogen. Subsequently, the $CD8^+$T-cell or DC becomes fully activated.

Initially, MHC-Class I obtains antigen fragments from the cytoplasm and presents them on the cell surface. Once activated, these cells begin to proliferate and can differentiate into cytotoxic T-cells (T_c) (Janeway et al., 2005). MHC Class I molecules are present on nucleated cells in the immune system, whereas MHC Class II molecules are not. However,

MHC Class II molecules are overwhelmingly present on T-cells, B-cells, and DCs. Additionally, they present antigen to $CD4^+$T-cells.

1.3.1 $CD8^+$T-cells

T-cell mediated immunity is integral in clearing intracellular bacterial infection (Lo et al., 1999). $CD4^+$T-cells are responsible for the recognition of exogenous antigens and are activated once pathogens have reached the vacuole of a cell (van der Velden et al., 2005). Conversely, $CD8^+$T-cells are responsible for the recognition of antigens and pathogens that enter the cytoplasm (van der Velden et al., 2005).

Previously, it has been shown that $CD4^+$T-cells are more important than $CD8^+$T-cells in acquired immunity to STm infection (Hughes and Galan, 2002). However, both $CD4^+$T-cells and $CD8^+$T-cells are intrinsic in orchestrating anti-microbial resistance (Lo et al., 1999). More specifically, $CD8^+$T-cells are instrumental for the instruction of pathogenic and/or cancerous cells to kill themselves via apoptosis.

Normally, $CD8^+$T-cells are rapidly activated in infections caused by intracellular pathogens and are recruited as part of the adaptive immune response (Tzelepis et al., 2012). However, in the case of virulent STm, which resides in macrophages, the activation of $CD8^+$T-cells is delayed in primary infection (Tzelepis et al., 2012, Luu et al., 2006, Mittrucker et al., 2002).

The functionality of $CD8^+$T-cells in the immune response is less clear and not well understood due to conflicting evidence from studies using different strains of STm. $CD8^+$T-cells have been suggested to be important in secondary (not primary) protection in the resolution of STm infection. This investigation, using the attenuated SL3261 strain

of STm, shows that $CD8^+$T-cells are important in both primary and secondary protection against STm.

1.3.2 CD8 DCs

Dendritic cells (DCs) are professional APCs on a majority of tissues that present antigens to naïve T-cells via MHC-Class I or II complexes in splenic T-zones (Banchereau and Steinman, 1998). They are key players in establishing bacterial immunity (Riquelme et al., 2012). However, STm can prevent DC-mediated activation of naïve T-cells and phagocytosis, thus preventing an adaptive immune response from occurring within the host (Riquelme et al., 2012).

Furthermore, DCs stimulate B and T-cells. B-cells recognize antigens directly via their B-cell receptor; however, T-cells need antigen presented to them via an APC, such as a DC (Banchereau and Steinman, 1998).

In this study, we will investigate DCs in the thymus. Mature DCs in the mouse model express MHC-class II, the co-stimulatory molecules CD40, CD80, and CD86, as well as CD11c, an integrin α-$_x$ chain, (Shortman and Liu, 2002). The T-cell markers, CD4 and CD8, are also present on mature DCs. Furthermore, CD8 or CD8α is an αα-homodimer, that is solely expressed on murine DCs and comprises about 70% of the thymus (Shortman and Liu, 2002). $CD8^+$ DCs play an important role in antigen presentation and T-cell priming in the immune response to STm (Shortman and Liu, 2002).

Three subsets of DCs have been found in the thymus (Li et al., 2009). They include: resident conventional DCs (cDCs), migratory cDCs, and plasmacytoid DCs (pDCs).

Plasmacytoid DCs (pDCs) ($B220^{+}CD11c^{+}$) comprise a subset of DCs that are responsible for producing IFN-γ, which plays an integral role in bacterial clearance during STm infection (Okada et al., 2003).

$CD103^{+}$ DCs (α_E) comprise a population of DCs that are present on all lymphoid and non-lymphoid organs (del Rio et al., 2010). It has been evidenced that twenty-three percent of STm reside within $CD11c^{+}CD11b^{-}$ DCs (Voedisch et al., 2009). Furthermore, STm has been found to reside within $CD103^{+}$ DCs and they have been associated with the uptake and presentation of STm in the mesenteric lymph node (MLN) of the gut (Voedisch et al., 2009).

1.4 Aims of the Study

The aim of this study is to use a CD8 knock out mouse model to characterise how the immune system responds to systemic STm infection in context of CD8 loss. The following question will be assessed:

1) How does STm infection impact the spleen, peritoneal cavity, and thymus in the absence of CD8 during the early (day 7) and later stages (day 35) of infection?
    a. What impact does CD8 loss have on the cellularity and architecture within each of these sites?

Chapter 2: Methods

2.1 Materials

Reagents and chemicals used in this study were obtained from Sigma-Aldrich (Poole, U.K.) unless stated otherwise.

2.2 Animals Used

Wild-type (WT) C57BL/6 mice were age and sex-matched between the ages of 6-12 weeks old and were obtained from HO Harlan OLAC Ltd. (Bicester, U.K). Transgenic mice, B6.129S2-Cd8a^{tm1Mak}/J or CD8 Knock-Out (KO) mice (as referred to in text), were bred from colonies maintained in the University of Birmingham Biomedical Services Unit (BMSU). The reference and original source is listed in Table 2.1. All animals were housed in the BMSU in specific-pathogen free conditions.

At specified times, mice were sacrificed by the Schedule 1 Method in compliance with United Kingdom (UK) Home Office (HO) guidelines. All experiments were carried out with ethical approval in accordance with the UK Ethics Committee.

Table 2.1: Knock-out mice used in the present study

Mouse Strain	Phenotype/Description	Original Source and Reference
B6.129S2-Cd8a^{tm1Mak}/J (CD8 KO)	This strain is deficient in functional cytotoxic T-cells	Donated by Dr. Nick Jones University of Birmingham Originally purchased from Jackson Laboratories (Fung-Leung et al., 1991)

2.3 Preparation of Antigens for Immunisation

2.3.1 Bacterial Strains

The attenuated *Salmonella enterica* serovar Typhimurium (STm) strain SL3261 is used throughout each infection (Hoiseth and Stocker, 1981).

Table 2.2: Bacterial strains used in the present study

Bacterial Strain	Description	Reference
SL3261	This strain is an attenuated auxotrophic mutant of *Salmonella* Typhimurium and is aro-A deficient.	(Hoiseth and Stocker, 1981)

2.3.1.1 Growth Conditions for SL3261 Bacterial Strain

STm was incubated overnight at 37°C with aeration (180 rpm) in sterile Luria-Bertani (LB) broth (recipe detailed in section 2.13) (Invitrogen, Paisley, UK) at and then diluted the next morning in LB broth and incubated as described but for 2 hours and grown until bacteria reached late-log phase (Optical Density (ODλ600 nm 0.9-1.0)).

Once the desired OD was reached, 1 mL of culture was transferred to an RNAse-free Eppendorf and harvested by centrifugation at 6,000 x g for 5 minutes at 4°C. Bacteria were washed twice in 1 mL sterile Phosphate Buffered Saline (PBS) at 6,000 x g for 5 minutes at 4°C and then re-suspended in 1 mL sterile PBS. The ODλ600 nm was measured again and the bacteria were diluted to a concentration of 5 x 10^8 bacteria per mL. Mice were infected with 5 x 10^5 bacteria by intraperitoneal injection (i.p.) in a final volume of 200 µL. The actual dosage of bacteria administered was calculated using the Miles and Misra CFU counting technique (Miles et al., 1938).

2.4 End-point of Infection

At specific time points of STm infection, mice were anaesthetised and peripheral blood was obtained via cardiac puncture. Mice were then sacrificed by cervical dislocation. All organs were obtained and removed under aseptic technique. Cells were extracted and isolated from the peritoneal cavity (PEC) for flow cytometry. The spleen and thymus were also removed and weighed for flow cytometry (spleen only), bacterial culture, cytokine analysis by ELISA (Enzyme-Linked Immunosorbent Assay), ELISpot (Enzyme-Linked Immunosorbent Spot Assay) , and immunohistochemistry (IHC).

2.5 Bacterial culture

The spleen and thymus (1 lobe per culture) were assessed for bacterial numbers after isolation. Tissues were weighed and then disaggregated in 1 mL of sterile RPMI-1640 medium through a 70 µm cell strainer (BD Biosciences) and were diluted by 10-fold serial dilutions in sterile RPMI-1640 medium. Bacterial serial dilutions (100 µL) were plated onto LB agar plates (detailed in section 2.14) and incubated overnight at 37°C.

Bacterial colonies were counted the following day and the total CFU per spleen or thymus lobe was calculated from the mass of the tissue section and dilution used.

2.6 Cell Preparation

2.6.1 Splenocyte Preparation

The spleen was disrupted in RPMI supplemented with 10% heat-inactivated foetal calf serum (FCS) and 1% penicillin/streptomycin (P/S) with subsequent disruption and filtration through a 70 µm cell strainer (BD Biosciences). Cells were then harvested and centrifuged at 175 x g for 4 minutes at 4°C. Erythrocytes/red blood cells (RBCs) were then lysed in sterile ACK Lysing Buffer (Gibco Invitrogen Compounds) as per manufacturer's guidelines. Cells were then washed in 5 mL of RPMI and centrifuged at 175 x g for 4 minutes at 4°C to remove any residual lysis buffer. Cells were then re-suspended in 10 mL RPMI and viable cell numbers were counted in order to obtain viable cell numbers using Trypan Blue staining to quantify live cells. Samples were then diluted to obtain an optimum cell density of 1.0×10^7 cells per mL.

2.6.2. Peritoneal Exudate Cells (PEC) Preparation

PEC cells were removed from the peritoneal cavity in 5 mLs of FACS (Flourescence Activated Cell Sorter) buffer (PBS containing 10% FCS and 2mM EDTA (Ethylenediaminetetraacetic acid solution) (Fluka Analytical, UK). Cells were then washed at 175 x g for 4 minutes at 4°C. If any samples contained RBCs, then they were lysed as per splenocytes. Cells were resuspended in 5 mL of FACS buffer and centrifuged at 175 x g for 4 minutes at 4°C to remove any residual lysis buffer and then re-

suspended in 5 mLs of FACS buffer in order to determine cell density as described in section 2.6.1.

2.7 Staining by Flow Cytometry

Extracellular staining of splenocytes and PEC suspensions was carried out for 25 minutes at 4°C in FACS buffer. The antibodies that were used are described in Table 2.3. Diluted cell samples were harvested (1 x 10^6) in a V-bottom 96-well plate (Corning Life Sciences, Netherlands) and centrifuged at 175 x g for 4 minutes at 4°C. Pelleted cells were washed in FACS buffer at 175 x g for 4 minutes at 4°C. Cells were then incubated with anti-CD16:CD32 antibody to block Fc receptors (CD32/FcγIII and CD16/FcγII receptors) prior to staining for 25 minutes at 4°C. Cells were then stained with the antibodies listed in Table 2.3. They were then washed with FACs buffer at 175 x g for 4 minutes at 4°C and re-suspended in FACS buffer for acquisition on a Cyan FACS Analyser in conjunction with Summit v4.3 software.

Analysis of extracellular and intracellular stained single-cell suspensions were conducted offline by FlowJo software 9.6.3(TreeStar).

Table 2.3 Antibodies used for Flow Cytometry Staining

Antibody	Clone	Dilution	Source	Target
Purified CD16:CD32	93	1:100	e-Bioscience	Blocks FcγII and FcγIII receptors
CD3 FITC	145-2C11	1:100	e-Bioscience	T-Cells
CD4 Pacific Blue		1:100		
CD44 PerCP-Cy 5.5	IM7	1:200	e-Bioscience	
CD62L PE	MEL-14	1:200	e-Bioscience	
CD19 APC -Cy7	ID3	1:200	BD Biosciences	B-Cells/Spleen and PEC
CD21 FITC	7G6	1:100	e-Biosciences	
CD23 PE	B3B4	1:100	e-Biosciences	
B220 PE Texas Red	RA3-6B2	1:400	BD PharMingen	
CD5 PerCP Cy 5.5	53-7.3	1:200	e-Biosciences	
IgM PE- Cy7	11/41	1:200	e-Bioscience	
IgD Pacific Blue	11-26c	1:200	e-Bioscience	
CD11b APC	MI-70	1:200	e-Bioscience	
CD138 PE	281-2	1:300	BD PharMingen	Plasma Cells (Extracellular)
B220 PerCP Cy 5.5	RA3-6B2	1:300	BD Bioscience	
CD19 APC	1D3	1:200	BD PharMingen	
IgG2b FITC	Polyclonal	1:500	Southern Biotech	
IgG2b Isotype FITC	N/A	1:500	BD PharMingen	
IgG2c FITC	Polyclonal	1:1000	Southern Biotech	
IgG2c Isotype FITC	RTK4174	1:1000	BioLegend	
CD69 FITC	H1.2F3	1:200	e-Bioscience	Thymocytes
CD4 Pacific Blue	RM4-5	1:100	e-Bioscience	
CD44 PerCP-Cy5.5	IM7	1:200	e-Bioscience	
CD45 APC-Cy7	30-F11	1:500	e-Bioscience	
CD25 APC	PC61.5	1:200	e-Bioscience	
TCR-β PE	H57-597	1:200	e-Bioscience	

2.8 Peripheral Blood

Peripheral blood was obtained by cardiac puncture at sacrifice. Blood was left to clot for one hour at 37°C and serum was separated from the clotted blood via centrifugation at 6000 x g for 15 minutes. Serum samples were then frozen and stored at -20°C until required for future ELISAs.

2.8.1 Enzyme-Linked Immunosorbent Assay (ELISA)

ELISA assays were performed against antigens including OMPs (outer membrane porins), purified porins, and LPS (lipopolysaccharide) (Alexis Biochemicals).

OMPs were prepared and obtained from Charlotte Cook (University of Birmingham, UK) (Henderson et al, 1997). Purified porins were obtained from Dr. Constantino López-Macías (Mexico Institute for Social Security, Mexico City, Mexico) as described in Section 2.3.2.

Serological antibody titres were confirmed and quantified for specificity against the antigens mentioned above. Nunc Maxisorp flat-bottomed 96-well plates (Thermo Fisher Scientific) were coated with 5 µg/mL of the antigen of interest at 4°C overnight. The antigen was diluted in ELISA Carbonate Coating Buffer (0.83 g Na_2HCO_3, 1.42 g NaH_2CO_3, 0.1% NaN_3 in 500 mL of double-distilled H_2O).

After coating, plates were washed with ELISA wash buffer (0.05% Tween-20 (Sigma, UK) in 1x PBS). After washing, plates were blocked for 1 hour at 37°C in ELISA blocking buffer (1% Bovine Serum Albumin (BSA) (Sigma) in 1x PBS in 500 mL of double-distilled H_2O). After blocking, plates were washed again in wash buffer and the primary antibodies (sera) were diluted in ELISA dilution buffer (0.05% Tween-20, 1% BSA in

500 mL of double-distilled H_2O) initially at 1:10, 1:20, or 1:50 dilutions and in subsequent four-fold serial dilutions. Plates were incubated for 1 hour at 37°C and then washed in wash buffer as before. Plates were then coated with alkaline phosphatase (AP)-conjugated antibodies (as described in Table 2.4) and incubated for 1 hour at 37°C. Plates were then washed for the last time in wash buffer and 100 µL of Sigma-Fast p-Nitrophenylphosphate substrate (pNPP and TRIS tablets, Sigma N2770) was added to each well as per the manufacturer's instructions. Plates were incubated with the substrate at 37°C until the desired colour change is obtained. Plates were read at λ405 nm using Softmax Pro software on an Emax Precision Microplate Reader (Molecular Devices) and the antibody titres were obtained.

Table 2.4 Antibodies used for ELISAs

Specificity	Dilution	Source
IgA	1:1000	Southern Biotech
IgG	1:1000	AbD Serotech
IgG1	1:1000	Southern Biotech
IgG2b	1:2000	Southern Biotech
IgG2c	1:1000	Southern Biotech
IgG3	1:1000	Southern Biotech
IgM	1:2000	Southern Biotech

2.9 Cytokine ELISA

Cytokines (IFN-γ and TNF-α) were detected by cytokine ELISAs. Splenocytes were diluted as per sample cell counts and 4 x 10^5 cells were plated per well (in triplicate) in sterile NUNC Maxisorb flat-bottomed 96 well plates coated overnight with anti-CD3 at 10 µg/well. Anti-CD28 (10 µg/well) were added to each well and incubated for 48 hours at 37°C. Supernatants were harvested and stored at -80°C until required for future ELISAs.

Table 2.5 Antibodies used for Cytokine ELISAs

Specificity	Clone	Dilution	Source	Application
Purified CD3e (No Azide)	17A2	1:100	e-Bioscience	Antibody used for Ex-Vivo Cytokine Re-Stimulation
Purified CD28 (No Azide)	JJ319	1:1000	BD Biosciences	
Purified IFN-γ	N/A	1:1000	e-Bioscience	Capture Antibody
IFN-γ Recombinant Protein	N/A	1:2000	e-Bioscience	Standard Antibody
Biotinylated IFN-γ	N/A	1:1000	e-Bioscience	Detection Antibody
Purified TNF-α	N/A	1:4000	e-Bioscience	Capture Antibody
TNF-α Recombinant Protein	N/A	1:1000	e-Bioscience	Standard Antibody
Biotinylated TNF-α	N/A	1:4000	e-Bioscience	Detection Antibody

NUNC Maxisorp 96-well plates were coated and sealed overnight at 4°C with 100 µL per well of capture antibody (IFN-γ and TNF-α) in 1x Coating Buffer (e-Bioscience) as outlined in Table 2.5. Following the overnight incubation, plates were washed five times in wash buffer (as described in Section 2.8.1)(Hoiseth and Stocker, 1981). Plates were then blocked with 200 µL of 1x Assay Diluent (eBioscience) and incubated for 1 hour at room temperature. After blocking, plates were washed in wash buffer four times. Standard antibodies were then diluted in 1x Assay Diluent as per Table 2.5 and 100 µL were added to each well. Two-fold serial dilutions were performed on the top standards (IFN-γ and TNF-α). Samples were initially diluted at 1:50 and two-fold serial dilutions were subsequently performed. Plates are then sealed and incubated overnight at 4°C. Following overnight incubation, plates were washed in wash buffer four times and then 100 µL of diluted detection antibody (Table 2.5) was added to each well and then sealed and incubated at room temperature for 1 hour. Following incubation, plates were

washed as described previously and 100 µL of diluted Avidin-HRP enzyme (1:4000) (eBioscience) was added to each well and then sealed and incubated for 30 minutes at room temperature. Plates were then washed as described previously. 1x TMB Substrate solution (eBioscience) (100 µL per well) was then added and incubated for 15 minutes at room temperature. Finally, 50 µL of Stop Solution (1M H_2SO_4) was added to each well. The plates were then read at an absorbancy of 450 nm using Softmax Pro software on an Emax Precision Microplate Reader (Molecular Devices) and the cytokine titres were obtained.

2.10 Histology

2.10.1 Tissue Freezing

Spleens and thymus tissues were cleaned under a dissecting microscope and then weighed and dissected into portions for freezing. One half of the spleen and one lobe of the thymus was snap frozen in liquid nitrogen and was stored at -80°C for analysis by immunohistochemistry (IHC).

2.10.2 Sectioning Tissue

To assess the pathogenicity of STm and subsequent immune response within the spleen and thymus, tissues were sectioned on a cryostat (Bright Instruments, Huntington, UK) using OCT TissueTek compound (Dako, Denmark). All sections were cut at a 5 µm thickness and mounted onto four-spot slides (CA Hendley Essex Ltd., Essex, UK). Sections were left to air-dry for 1 hour before fixation in acetone for 20 minutes at 4°C. Slides were air-dried overnight and then stored in polythene bags at -20°C until required for immunohistochemistry.

2.10.3 Immunohistochemistry (IHC)

Slides were thawed and re-hydrated in Tris buffer (pH 7.6) (1.0 L 200 mM Tris Base, 1.5 L 154 mM Physiological NaCl, 1.0L of 0.1 N HCl. Primary antibodies (Table 2.7) were diluted in Tris buffer (pH 7.6) and 75 µL of the appropriate antibody was added to each spot on the section slides. Sections were incubated for 1 hour at room temperature in a moist chamber and then washed twice in Tris buffer (7.6) for 5 minutes. Secondary antibodies conjugated with horse-radish peroxidase (HRP) or biotin (Bt) (Table 2.7) were pre-adsorbed in 10% normal mouse serum (NMS) and then made up to the correct volume in Tris buffer (pH 7.6) prior to addition to the slides. Slides were then incubated in a moist chamber for 45 minutes. Goat anti-hamster IgG (heavy and light chains) was added to the secondary antibody solution only prior to the addition of the 75 µL secondary antibody cocktail to the section only if hamster anti-mouse primary antibodies were used in the staining protocol. Following the incubation period, slides were washed twice in Tris buffer (pH 7.6) as before.

Alkaline phosphatase (AP) (AB Complex, Vector Laboratories, CA, USA) complex was pre-absorbed by the addition of equal amounts of A (avidin) and B (biotinylated AP) at a 1:100 dilution for 30 minutes. 75 µL was added to slides which were then incubated at room temperature for 40 minutes and then washed twice as before in Tris Buffer (pH 7.6).

Slides were then developed as follows. One peroxidase substrate , 3,3´-diaminbenzidine tetrahydrochloride (DAB) tablet was dissolved in 15 mL of Tris buffer (pH 7.6). The substrate was filtered immediately and one drop of hydrogen peroxide was added. The substrate was used immediately by adding one drop to each section. The substrate was

left to develop until the desired level of stain intensity was reached. Slides were individually washed as before in Tris buffer (pH 7.6).

Slides were then developed with the AP substrates (napthol AS-MX phosphate and Fast Blue BB salt). Levamisole (8 mg) was dissolved in 10 mL Tris buffer (pH 9.2) in order to inhibit endogenous phosphate activity. Napthol AS-MX phosphate (4 mg) was dissolved in N,N- dimethyl-foramide (380 μL) in a glass bottle in a fume hood. This solution was then added to the middle of the Levamisole [(-) tetramisole hydrochloride] solution in order to avoid a reaction with the plastic universal tube. Fast Blue BB salt (10 mg) was then added to the solution and then filtered immediately prior to the addition to slides. A single drop was added to each section until the desired level of stain intensity was reached. Slides were were washed in Tris Buffer (pH 7.6) as before and then washed twice in distilled H_2O to inhibit any further reaction of the substrates. Slides were then left to air-dry overnight and were mounted in the morning using Glycerol Gelatin (Sigma).

Photographs of desired areas of spleen and/or thymus sections were then taken using a Leica CTR6000 microscope (Leica, Milton Keynes, UK), QCapture software, and Image J for processing.

Table 2.6 Antibodies used for Immunohistochemistry

Antibodies	Isotype	Dilution	Source
Primary Antibodies			
B220	Rat anti-mouse	1:200	BD Pharmingen
CD103	Rat anti-mouse	1:200	BD Pharmingen
CD11c	Hamster anti-mouse	1:500	AbD Serotech
CD3	Rat anti-mouse	1:500	AbD Serotech
CD3e	Hamster anti-mouse	1:300	BD Pharmingen
CD4	Rat anti-mouse	1:800	BD Pharmingen
F4/80	Rat anti-mouse	1:400	AbD Serotech
IgA	Rat anti-mouse	1:200	BD Pharmingen
IgD	Sheep anti-mouse	1:800	AbCam
IgG	Rat anti-mouse	1:300	AbD Serotech
IgG2b	Rat anti-mouse	1:200	BD Pharmingen
IgG2a	Rat anti-mouse	1:250	BD Pharmingen
IgG3	Rat anti-mouse	1:200	AbD Serotech
IgM	Rat anti-mouse	1:300	AbD Serotech
IgM	HRP-Goat anti-mouse	1:50	Southern Biotech
PNA	Bt-Peanut Agglutinin	1:200	BD Pharmingen
Secondary Antibodies			
Donkey anti-Sheep Peroxidase (Px)	Donkey anti-sheep	1:300	Jackson Laboratories
Goat anti-Hamster IgG (heavy and light chains)	Goat anti-hamster	1:100	Southern Biotech
Rabbit anti-Rat Biotin (Bt)	Rabbit anti-rat	1:600	Dako

2.11 Statistical Analysis

Statistical analyses were performed using GraphPad Prism version 5. The statistical analysis of the results was determined by the Mann-Whitney U non-parametric sum of ranks test. A value of $P \leq 0.05$ was considered statistically significant. Experiments were repeated with significant findings indicated in the figure legends.

2.12 Media and Buffers

LB Agar Plates

20 g of Granulated Agar (Melford Laboratories, Ipswich, UK) and 20 g of LB Broth Base powder (Invitrogen) were dissolved in 1L distilled H_2O and autoclaved at 121°C for 30 minutes. Agar plates were poured in a fume hood whilst the agar was still warm and were dried at room temperature for a couple of hours. Plates were stored at 4°C until required.

LB Media

20 g LB Broth Base powder (Invitrogen, Paisley, UK) was dissolved in 1L distilled H_2O and autoclaved at 121°C for 30 minutes. The media was cooled down to room temperature prior to use.

Chapter 3: Results

3.1 Period of infection

Mice were infected as described in section(s) 2.3.1.1 and 2.3.2 and sacrificed on days 0,7, and 35 post-infection. These days were chosen in order to characterise the response of STm to WT and CD8 KO mice in the spleen, PEC, and thymus during the early (Day 7) and late (Day 35) stages of infection.

3.2 STm infection induces a multi-organ response

After sacrifice, WT and CD8 KO spleens, thymus, and peritoneal exudate cells (PEC) were extracted in order to characterise the extent of STm infection during a systemic NTS infection at days 0, 7, and 35 post-infection. The host mounts a successful immune response against STm infection within the first week; however, it is not effective in establishing sterile immunity. Subsequently, the adaptive immune response is established by days 18-21 and resolution should occur by day 35 post-infection. Initially, we set out to investigate the role of CD8 loss in the thymus during systemic *Salmonella* infection; however, we found that it contributed to a multi-organ response in other areas such as the spleen and peritoneal cavity.

3.3 The Spleen

3.3.1 Splenomegaly is induced within the host and severely disrupts the architecture of the spleen during the course of STm infection.

Splenomegaly was observed within the host at day 7 in both WT and CD8 KO (Figure 3.1a) and decreased in both groups of mice at day 35 (Figure 3.1b). This is equally correlated with the levels of bacterial burden within the tissue (Figure 3.2). However, the bacterial burdens within CD8 KO mice at day 35 post-infection are still elevated in contrast to WT mice (Figure 3.2a)(*,P=0.0286) .

Splenomegaly severely disrupts the architecture of the spleen in both WT and CD8 KO mice (Figure 3.3). At day 0, the white pulp (WP) and red pulp (RP) are clearly defined, along with the MZ, B-cell follicles, and T-zone areas. By day 7, there is a distinct lack of organization within the spleen. The MZ has disappeared and there is a loss of distinction between the red pulp and the white pulp. By day 35, GCs appear and are present within the spleen.

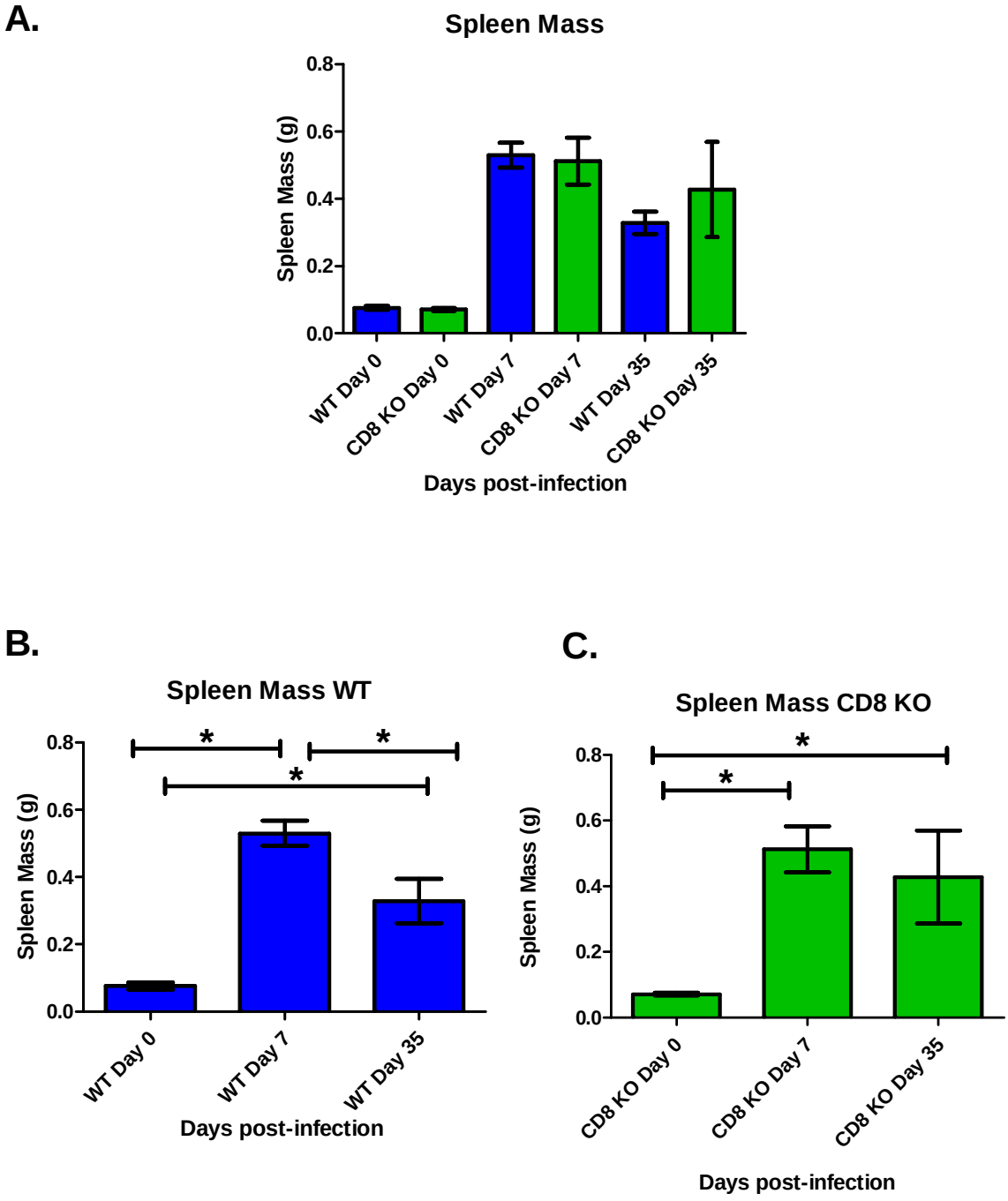

Figure 3.1 Changes in splenic mass occur over the course of STm infection. (A) Splenomegaly was observed by day 7 post-infection in both WT and CD8 KO mice and decreased as resolution of STm infection occurred. (B) Spleen mass of WT mice (C) Spleen mass of CD8 KO mice. Data is taken from one experiment where n=4. The Mann-Whitney U test was used to confirm statistical significance. Data represented as mean ±SEM. * represents statistically significant data ($P<0.05$)

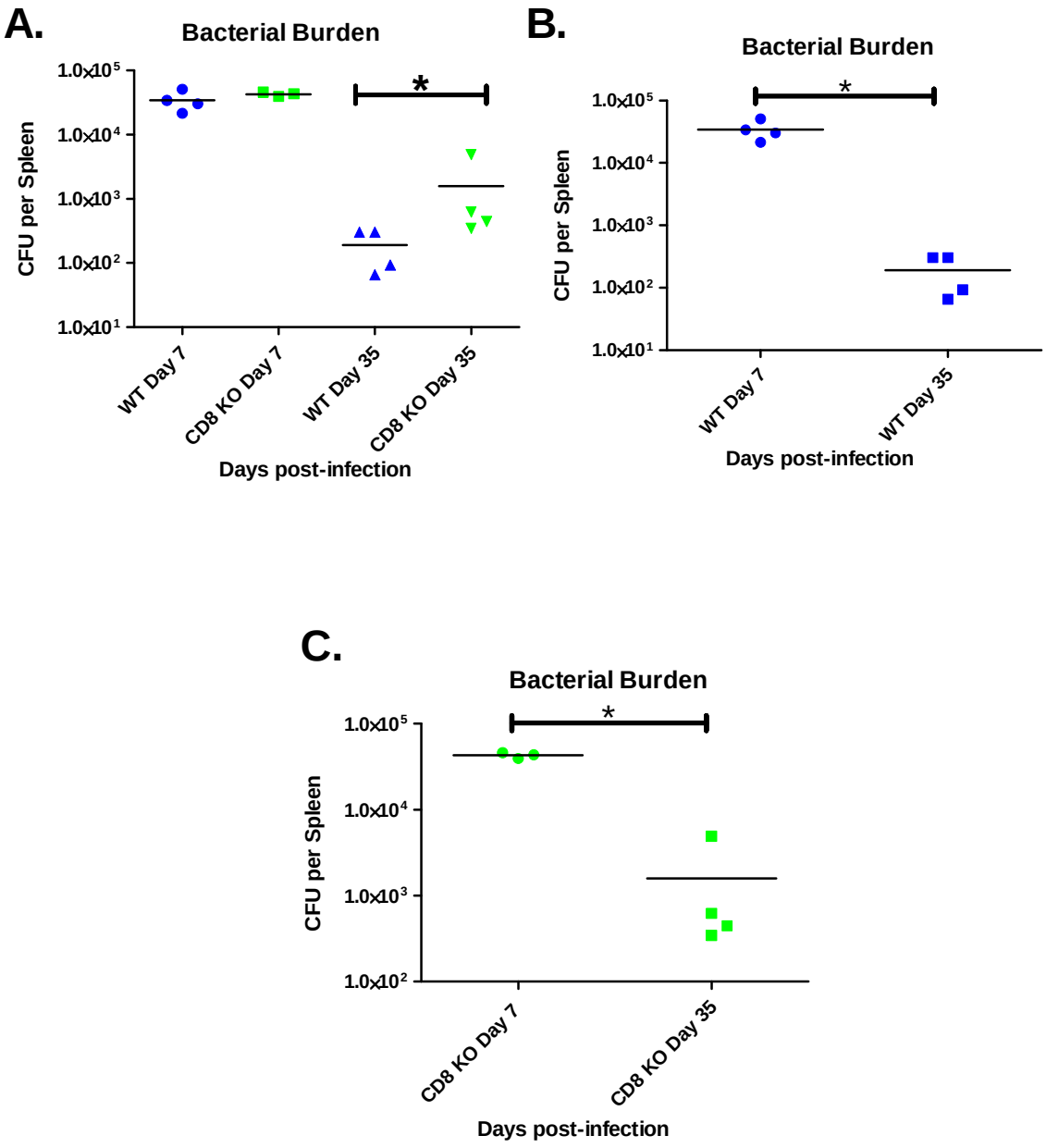

Figure 3.2. Bacterial burdens are highest at day 7 post -infection and decrease by day 35 post -infection. Bacterial burdens are directly proportional to spleen weights during the first week of STm infection. (A) Comparison of bacterial burden between WT and CD8 KO mice at days 7 and 35 post -infection. (B) WT bacterial burden at days 7 and 35 post -infection. (C) CD8 KO bacterial burden at days 7 and 35 post -infection. Data is taken from one experiment where n=4 , except for the CD8 KO mice group at day 0 wh ere n=6. The Mann-Whitney U test was used to confirm statistical significance. Horizontal bars represent means . * represents statistically significant data (P<0.05) .

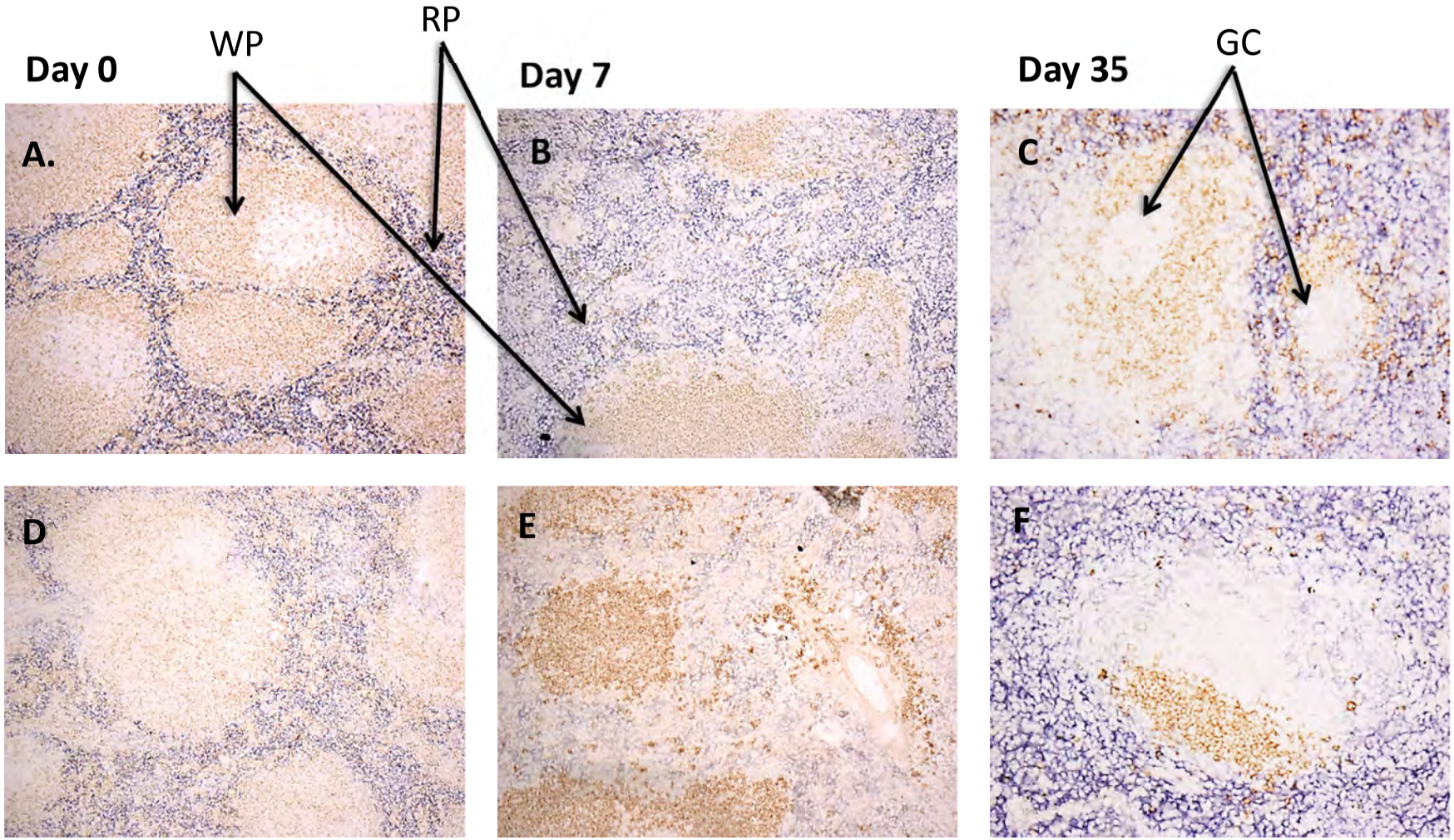

Figure 3.3 Immunohistochemistry staining for F4/80 (blue) and IgD (brown) during days 0,7, and 35 post-STm infection (A,B,D,E-X10 image)(C,F-X20 image) (A-C) WT mice (D-F) CD8 KO mice. Blue areas= red pulp (RP), brown areas= white pulp (WP), GCs are absent in days 0 and 7, but are present at day 35.

3.3.2 Flow cytometric analysis

3.3.2.1 Splenic T-cell populations

In addition to visualizing the spleen via IHC, there were no significant differences seen between WT and CD8 KO mice in the number of $CD4^+$T-cells, $CD3^+CD4^+$T-cells, effector cells (CD620loCD44hi), and naïve cells (CD62hiCD44lo) (Figure 3.4). However, one can still detect subtle increases in the expanded T-cell populations from day 0 to day 7 , as depicted in Figure 3.4.

3.3.2.2 Splenic B-cell populations

Splenic B-cell populations were also assessed for their distinct phenotypes. Follicular, MZ, and transitional populations were gated on $B220^+$ and IgM^+. There were no apparent differences seen between WT and CD8 KO follicular and MZ B-cell populations gated on $B220^+$ and IgM^+ (Figure 3.5). However, there were statistically significant differences seen between WT and CD8 KO transitional B-cell populations gated on $B220^+$ (*,P=0.0381) and IgM^+ (*, P=0.0381) at day 0.

3.3.2.3 Splenic plasma cell populations

Splenic plasma cell populations were also assessed for an $IgG2b^+$ or $IgG2c^+$ phenotype. These populations were gated on $B220intCD19intCD138^+$ and $CD138^+$, respectively. There were no statistically significant differences seen between WT and CD8 KO plasma cell populations (Figure 3.6).

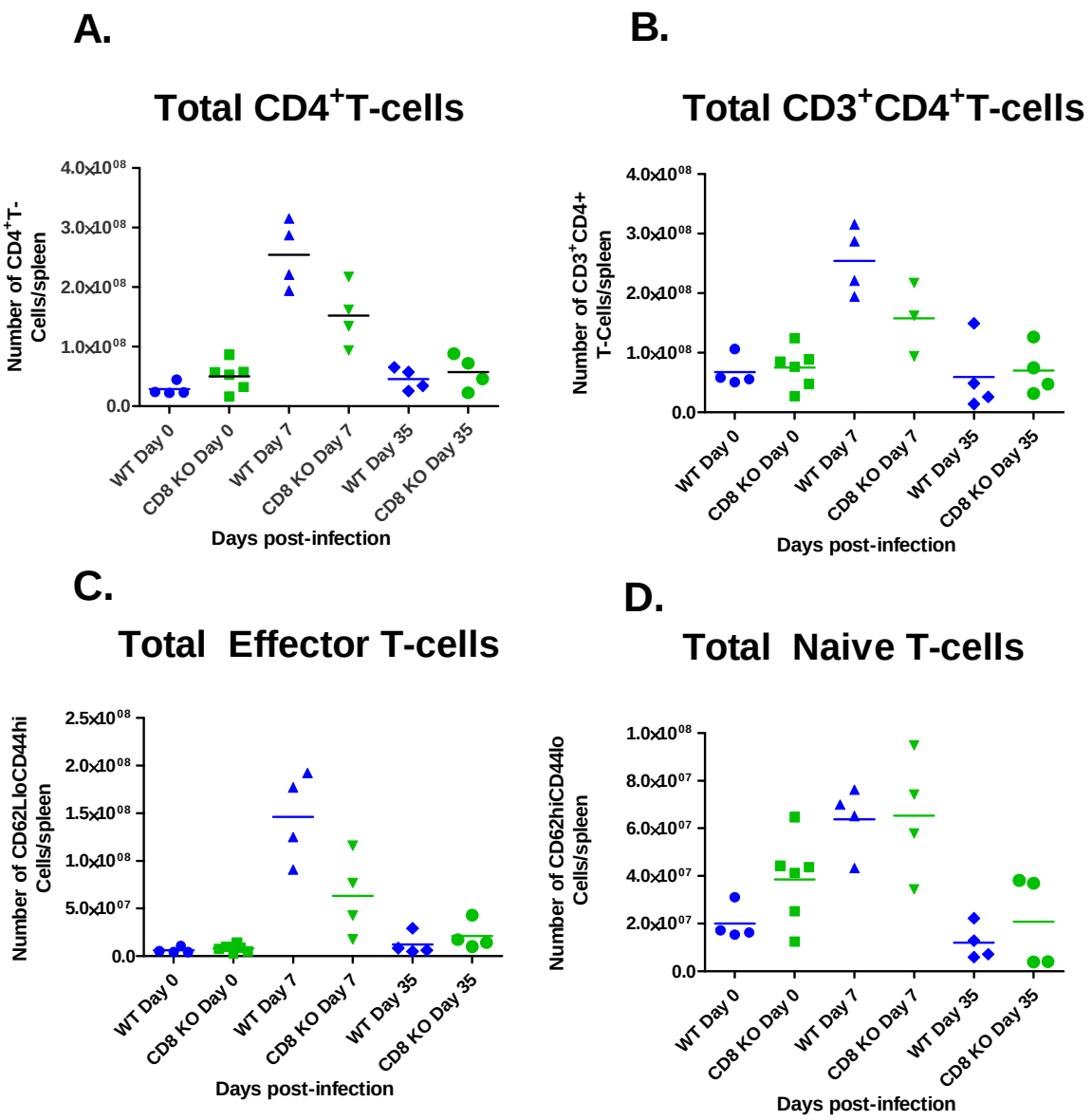

Figure 3.4 Splenic T-cell population changes over the course of STm infection (WT vs CD8 KO- day 0, 7, and 35) Data is taken from one experiment where n=4. The Mann-Whitney U test was used to confirm statistical significance. Horizontal bars represent means. * represents statistically significant data ($P<0.05$).

3.3.3 Antigen-specific antibodies can be detected by ELISAs and immunohistochemistry (IHC) within the spleen

Serum IgM and IgG were detected by ELISAs against outer membrane proteins (OMPs) and this could be visualised by immunohistochemistry (IHC). Lower levels of OMP-specific IgG antibody were detected in the spleens of CD8 KO mice (Figure 3.7b) in contrast to WT (Figure 3.7a) on day 7 post-infection and this was quantified by ELISA (Figure 3.7c) (*,P=0.0270). Normal levels of OMP-specific IgM antibody were detected in both WT and CD8 KO mice, which was visualised by IHC (Figure 3.8a/b) and quantified by ELISA (Figure 3.9c) at day 7 post-infection and persisted at day 35 during STm infection. The lower levels of IgG did not persist within the CD8 KO mice and levels returned to normal at approximately day 35 (Figure 3.9) (pictures not shown).

Furthermore, serum IgG2b$^+$ and IgG2c$^+$ antibody can be detected via ELISAs and IHC (Figure 3.10 and 3.11, respectively). Lower levels of IgG2b antibody were detected in the spleens of CD8 KO mice by ELISA (*,P=0.0210) (Figure 3.10g) and can be visualised by IHC, particularly at day 7 post-infection (Figure 3.10d). However, IgG2b antibody titres were seen to increase substantially in both WT and CD8 KO mice from day 0 to day 7 post-infection (data not shown). IgG2b antibodies were also seen at day 35 post-infection (Figure 3.10e and 3.10f). However, there were no differences found in the levels of IgG2c antibody titres by ELISA (P=0.0627), but there seems to be a lower trend in the quantity of IgG2c antibody in CD8 KO mice (Figure 3.11c). However, this was quite difficult to visualize by IHC and no significant differences were seen by staining (Figure 3.11a and 3.11b).

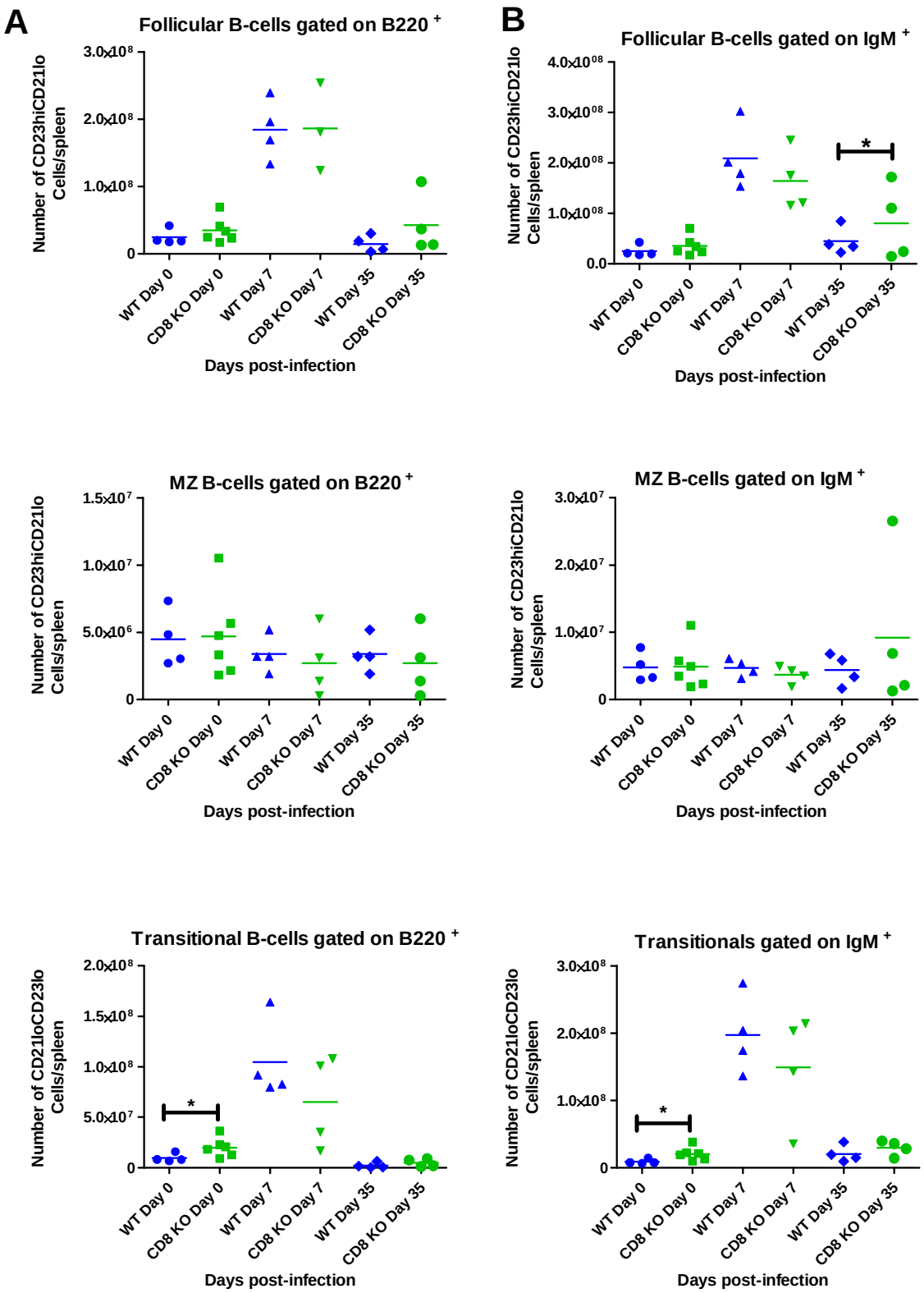

Figure 3.5 Splenic B-cell populations gated on (A) B220$^+$ and (B) IgM$^+$ Data is taken from one experiment where n=4. The Mann-Whitney U test was used to confirm statistical significance. Horizontal bars represent means. * represents statistically significant data ($P<0.05$)

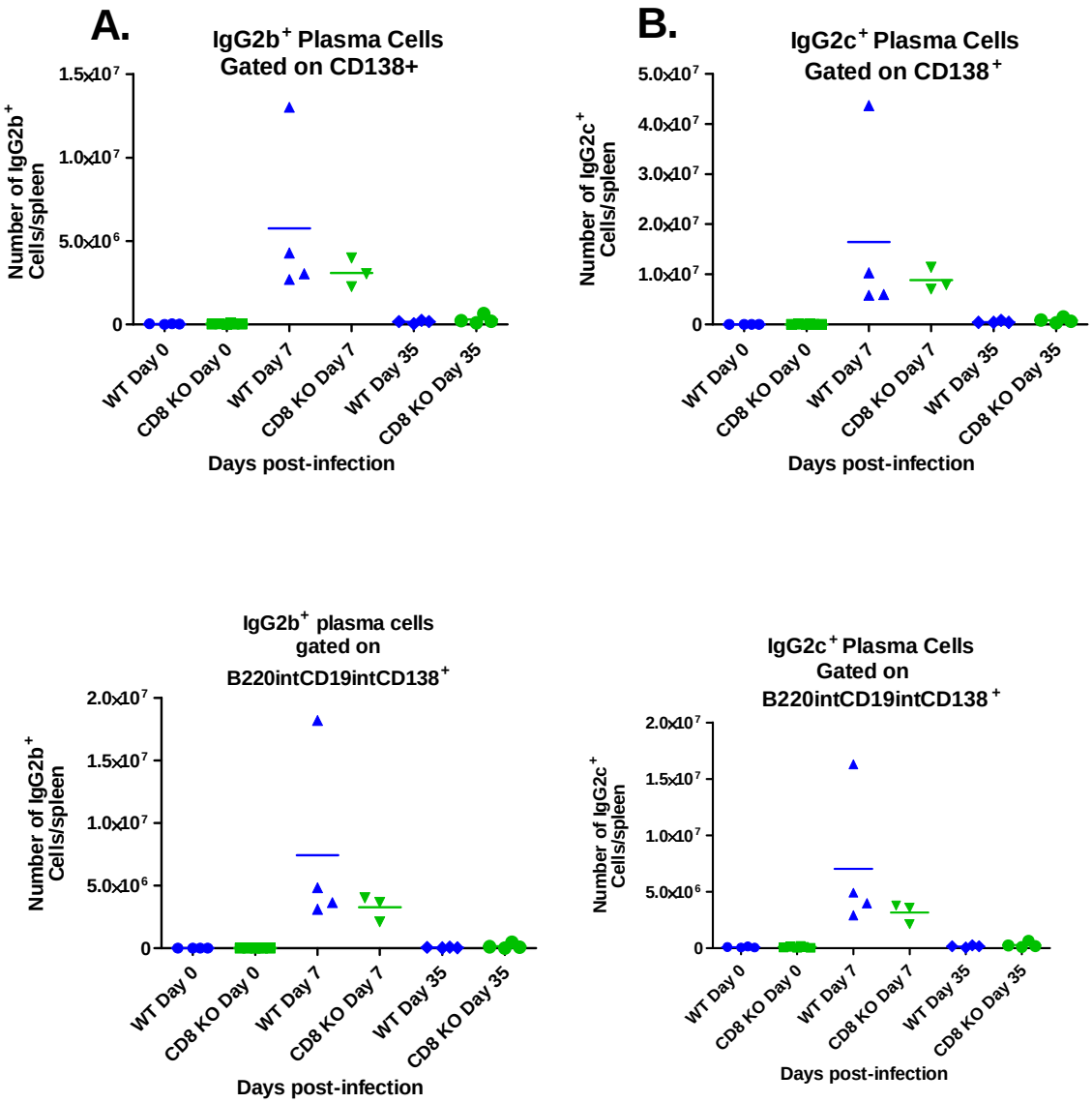

Figure 3.6. IgG2b$^+$ (A) and IgG2c$^+$ (B) splenic plasma cell populations. Data is taken from one experiment where n=4. The Mann-Whitney U test was used to confirm statistical significance. Horizontal bars represent means. * represents statistically significant data ($P<0.05$).

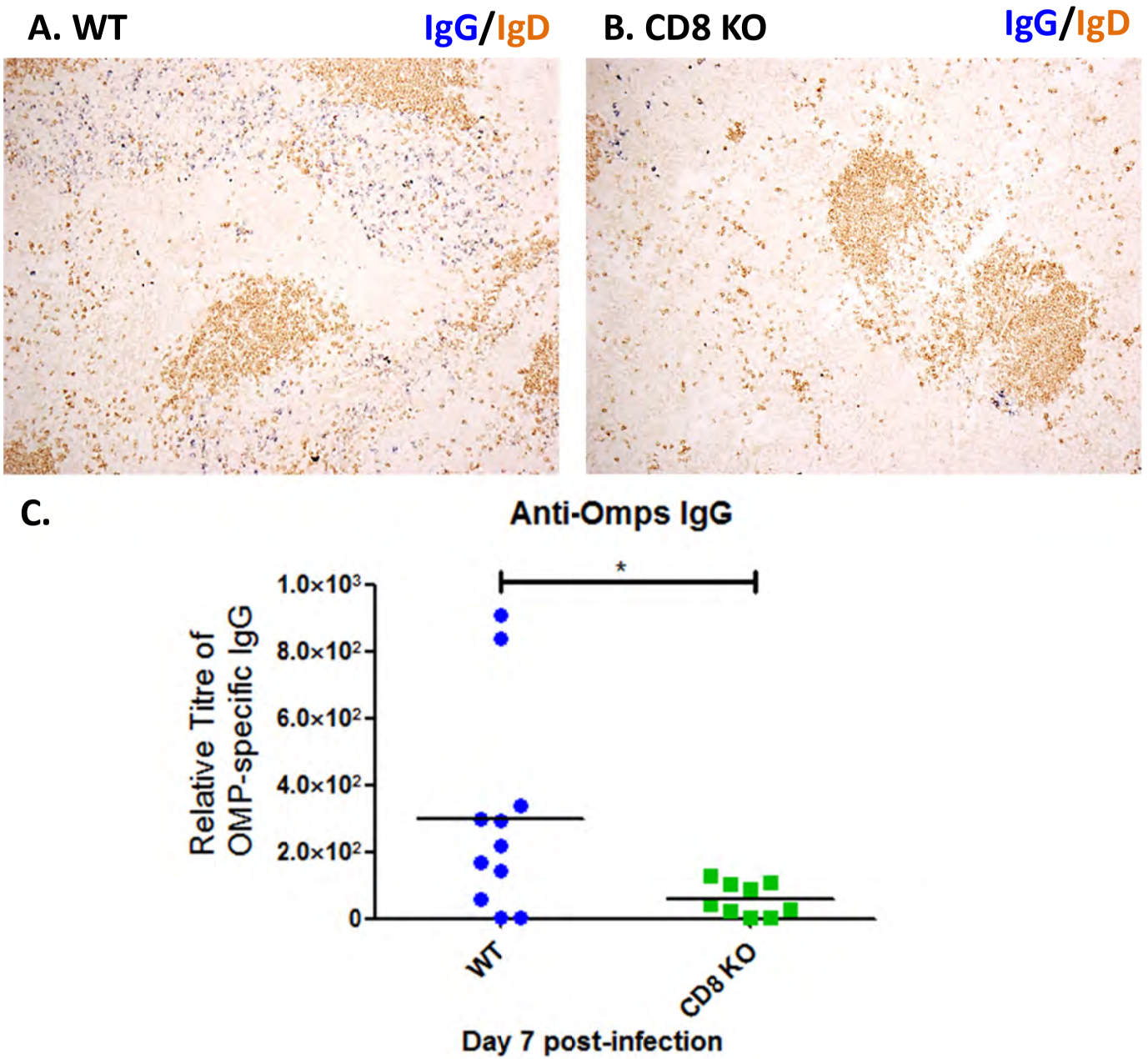

Figure 3.7. Differences in the OMPs-specific IgG antibody response can be detected in the spleen via IHC (x10 images) (A and B) and ELISA. Serum IgG titres (C) were assessed from WT (A) and CD8 KO (B)mice by ELISA against OMPs. Data is representative of three-independent experiments and 4 mice per group. *P≤0.05. The Mann-Whitney U test was used to compare the statistical significance between groups .

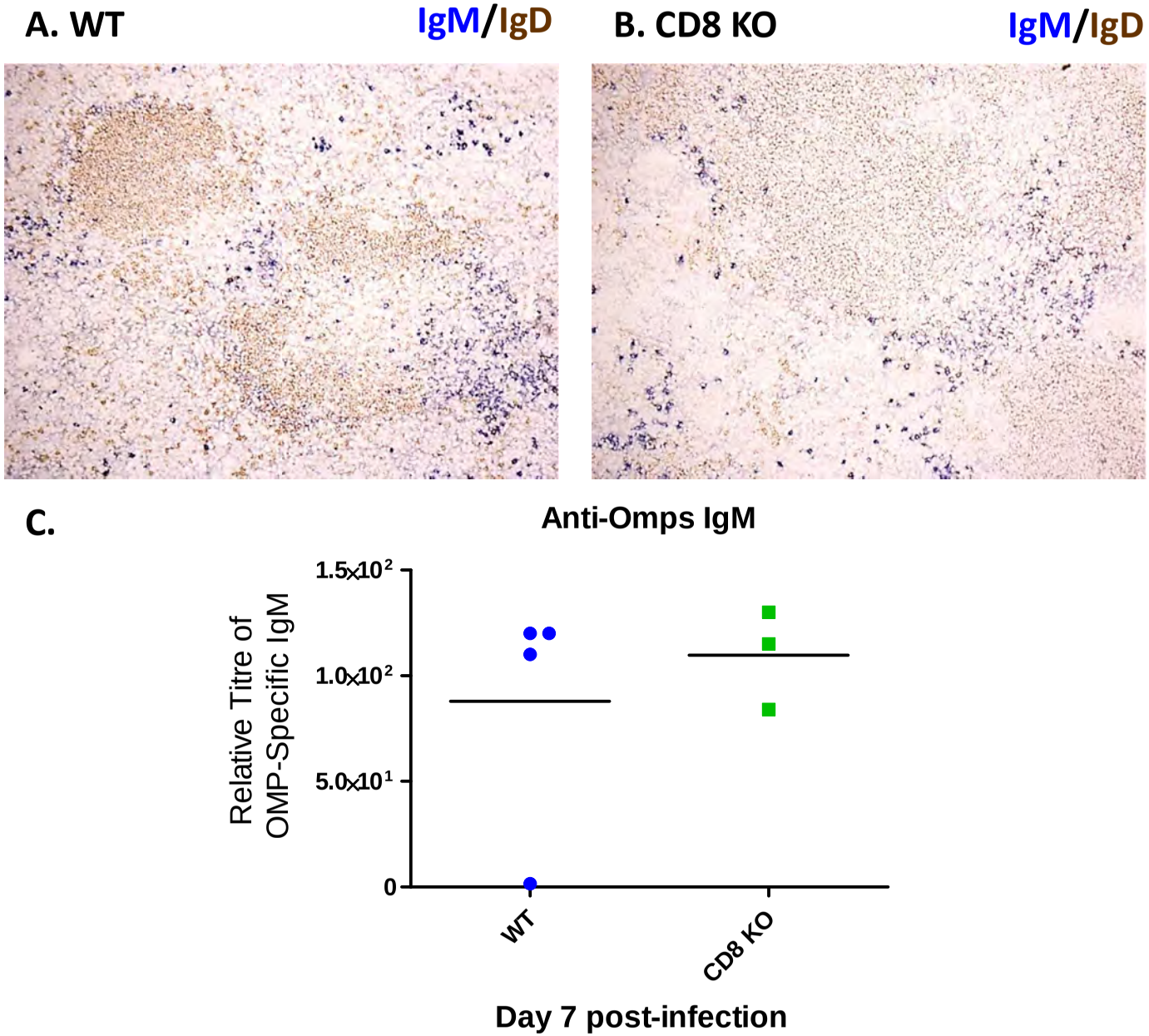

Figure 3.8. No differences in the OMPs-specific IgM antibody response can be detected in the spleen via IHC (x10 images) (A and B) and ELISA. Serum IgM titres (C) were assessed from WT (A) and CD8 KO (B)mice by ELISA against OMPs. Data is representative of one experiment and 4 mice per group. *P≤0.05. The Mann-Whitney U test was used to compare the statistical significance between groups.

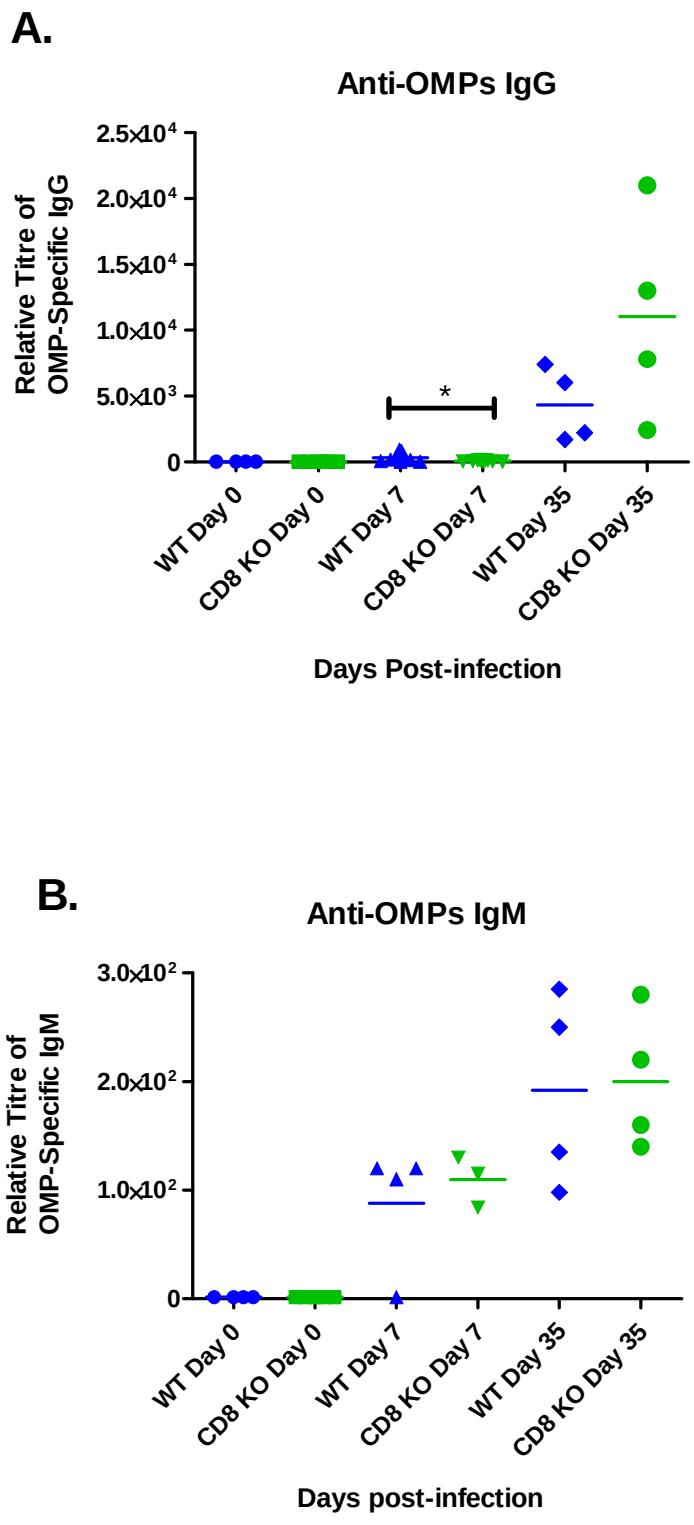

Figure 3.9. Relative antibody titres of OMP-specific IgG (A) and IgM (B) in WT and CD8 KO mice post-infection with STm. Serum anti-OMPs antibody titres were quantified by ELISA. Data is representative of 4 mice per group in both A and B apart from Day 7 WT and CD8 KO mice in (A), which reflects 3 independent experiments. Horizontal bars reflect means. *P≤ 0.05.

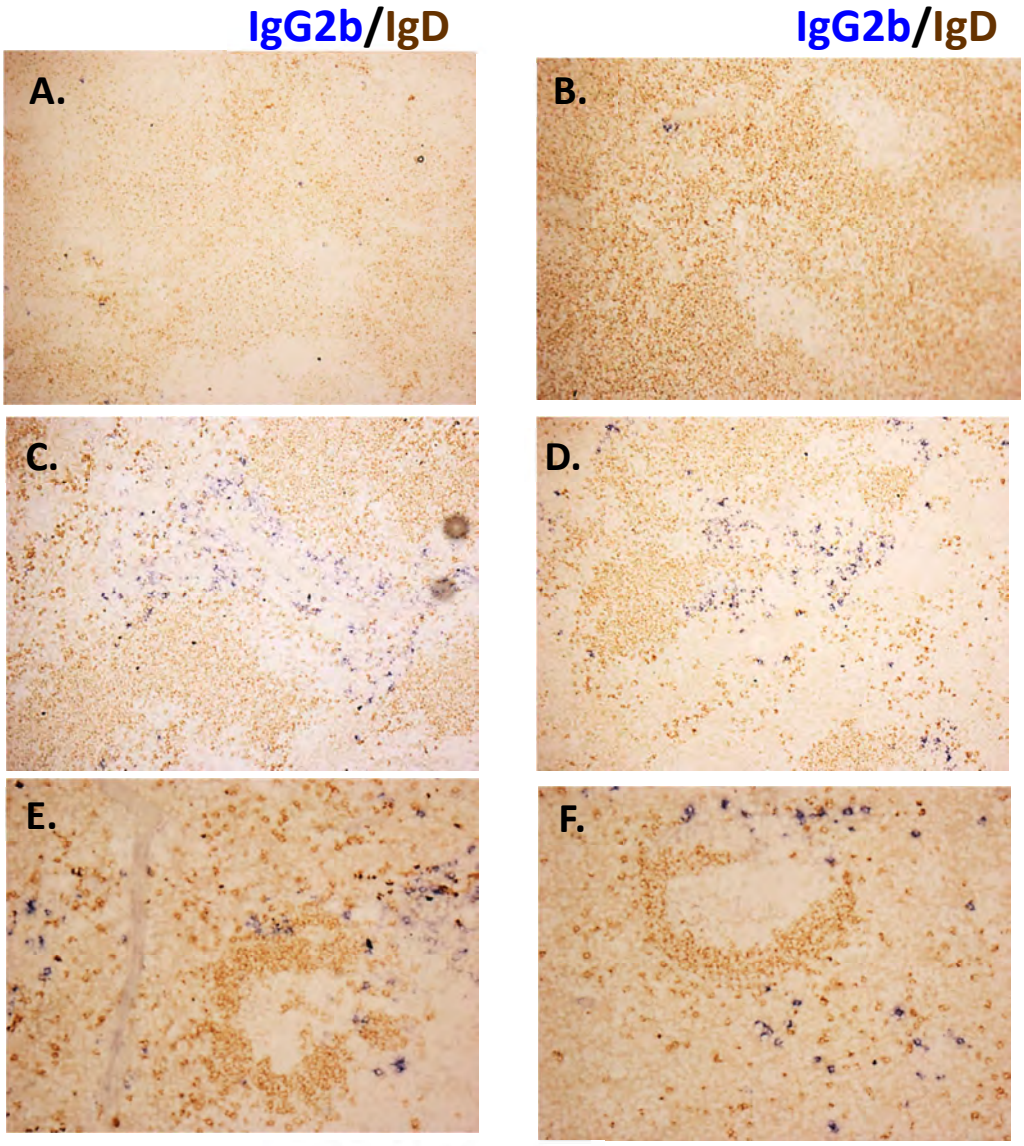

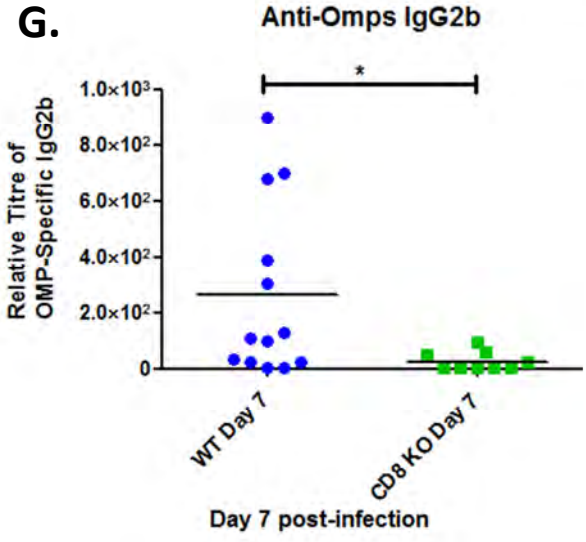

Figure 3.10. Differences in the antigen-specific IgG2b antibody response can be detected in the spleen via IHC (x10 images-A –D) (x20 images E-F) and ELISAs (Day 7) (G). IgG2b antibody levels were visualised by IHC in WT and CD8 KO mice, respectively on day 0 (A-B), day 7 (C-D), and day 35 (E-F). Serum IgG 2b titres (G) were assessed from WT (C) and CD8 KO (D) mice by ELISA against OMPs. Horizontal bars represent means. Data is representative of three-independent experiments and 4 mice per group. *P≤0.05. The Mann-Whitney U test was used to compare the statistical significance between groups .

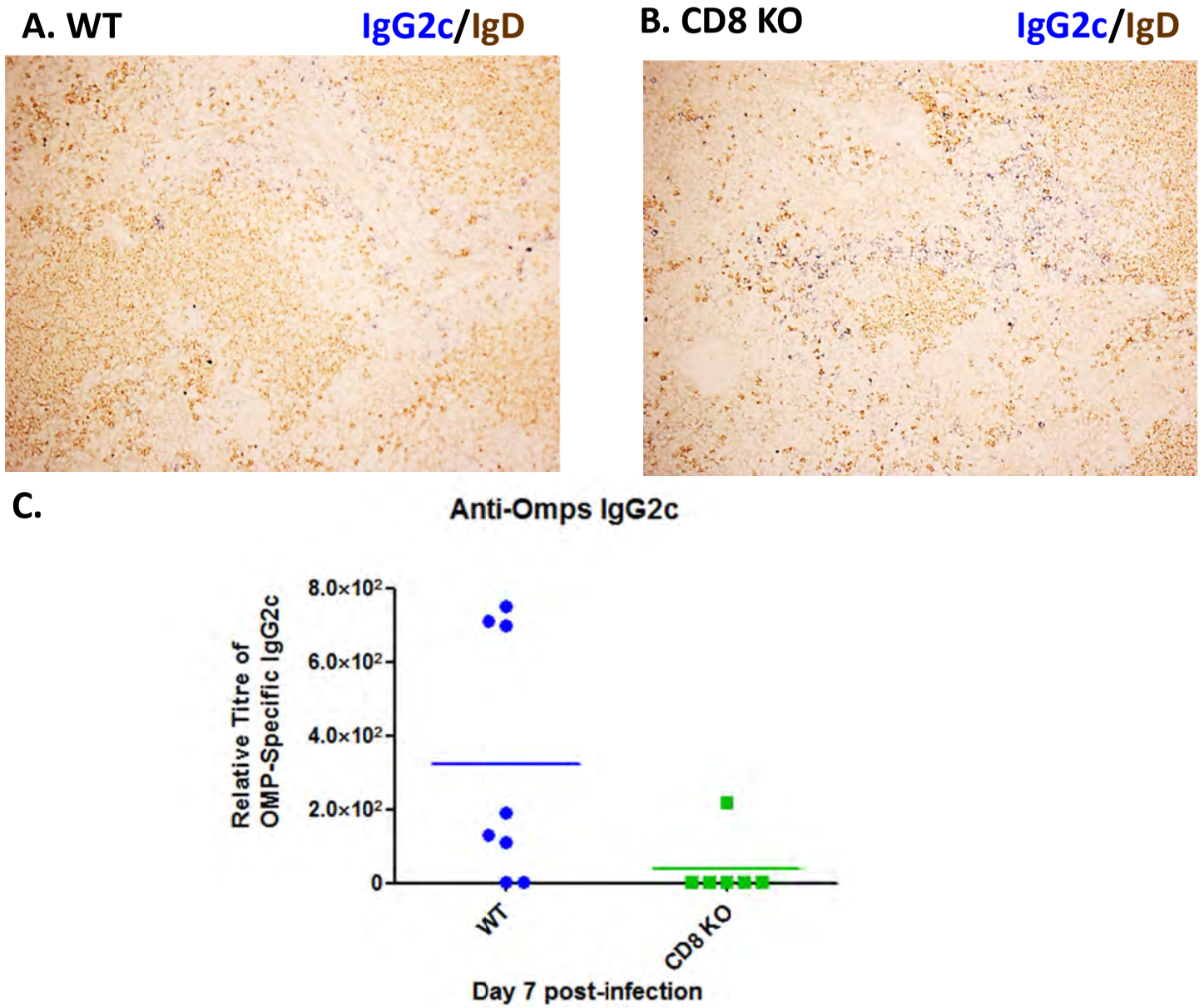

Figure 3.11. No differences in the OMPs-specific IgG2c antibody response can be detected in the spleen via IHC- Day 7 post-infection (x10 images) (A and B) and ELISA (C) . Serum IgG2c titres (C) were assessed from WT (A) and CD8 KO (B)mice by ELISA against OMPs. Horizontal bars represent means. Data is representative of two experiments and 4 mice per group. *P≤0.05. The Mann-Whitney U test was used to compare the statistical significance between groups.

3.4 The Peritoneal Cavity

The peritoneal cavity was assessed for B1b cells. There were no significant differences seen between WT and CD8 KO mice on days 7 and 35; however, there was a significant difference found on day 0 (*,P=0.0190) (Figure 3.12).

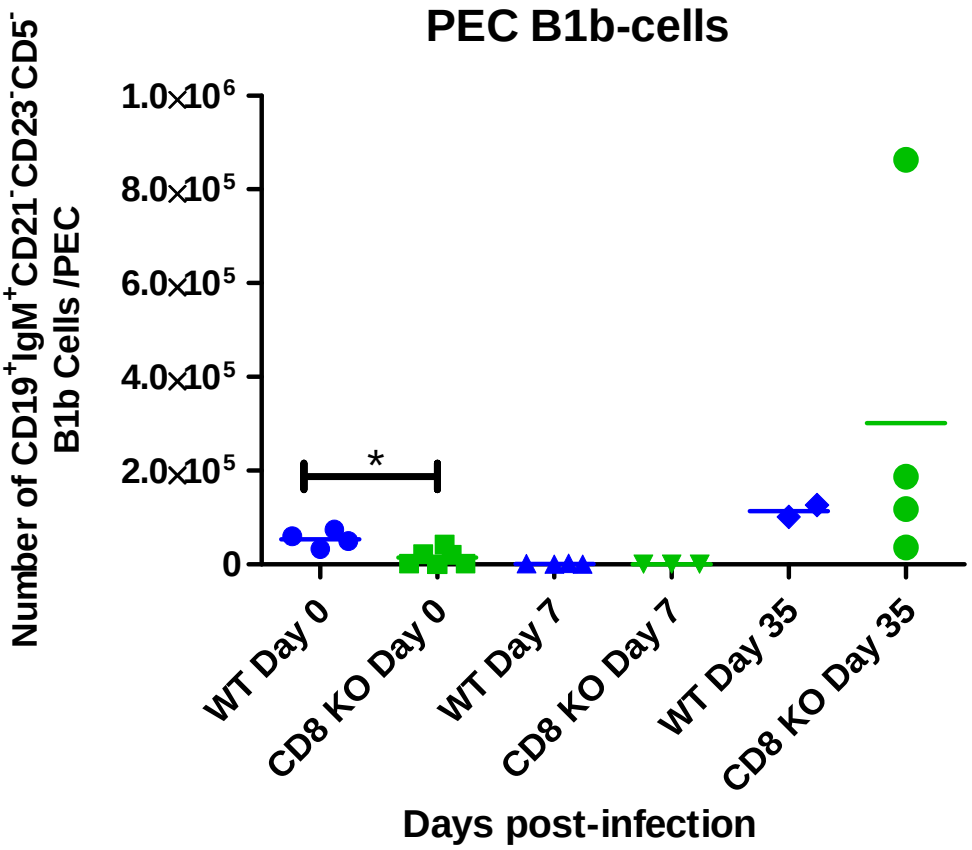

Figure 3.12. B1b cells within the peritoneal cavity. Data is taken from one experiment where n=4. The Mann-Whitney U test was used to confirm statistical significance. Horizontal bars represent means. * represents statistically significant data (P<0.05).

3.5 The Thymus

3.5.1 Thymic atrophy is induced over the course of STm infection

Thymic atrophy is induced over the course of STm infection and is reflected by its mass size at day 7 post-infection in both WT and CD8 KO mice (Figure 3.13). There were no significant differences in thymic mass nor bacterial burden (Figure 3.14) between both groups , thus, bacterial culture was not performed on the thymus at day 35 post-infection.

3.5.2 Thymic DCs

Thymic DCs play an integral role in the uptake and presentation of STm i.e. the MLN before migrating to the thymus (Voedisch et al., 2009). In the periphery, DCs that reside in the intestinal epithelium are known to internalise STm and then infect macrophages in the submucosa (Ibarra and Steele-Mortimer, 2009). Thus, IHC was performed to visualise thymic macrophages ($F4/80^{+}CD11c^{+}$) (Figure 3.15), pDCs (Figure 3.16) , and $CD103^{+}$DCs (Figure 3.17).

Thymic DCs were very rare and difficult to visualise with IHC, thus, there were no differences found in the number nor type of DCs in WT and CD8 KO mice.

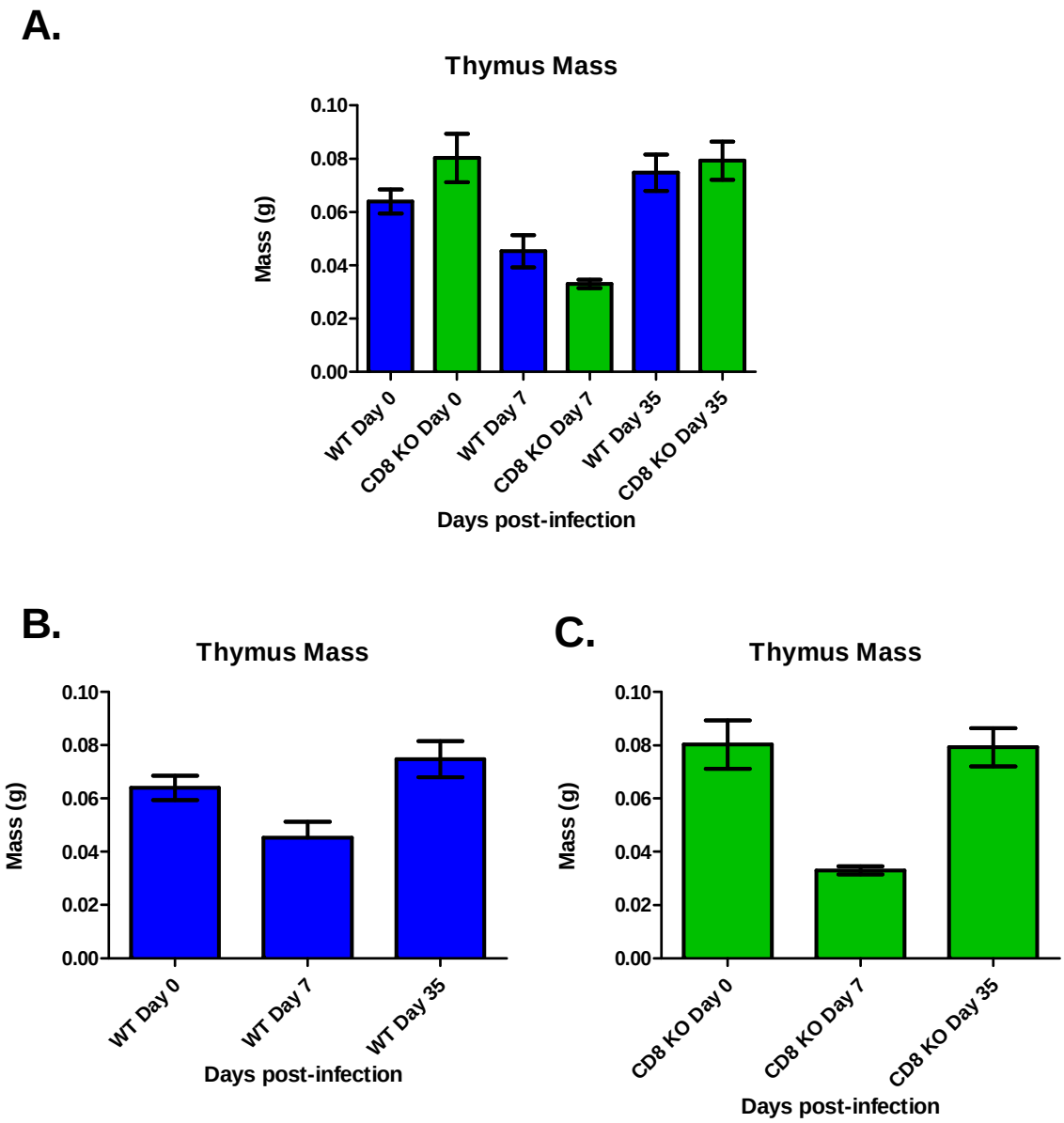

Figure 3.13. Changes in thymic mass occur over the course of STm infection. (A) Thymic atrophy was observed by day 7 post-infection in both WT and CD8 KO mice and resolved as bacterial clearance was enhanced by day 35. (B) Thymic mass of WT mice (C) Thymic mass of CD8 KO mice. Data is taken from one experiment where n=4. The Mann-Whitney U test was used to confirm statistical significance. Data represented as mean $\pm$SEM. * represents statistically significant data ($P<0.05$).

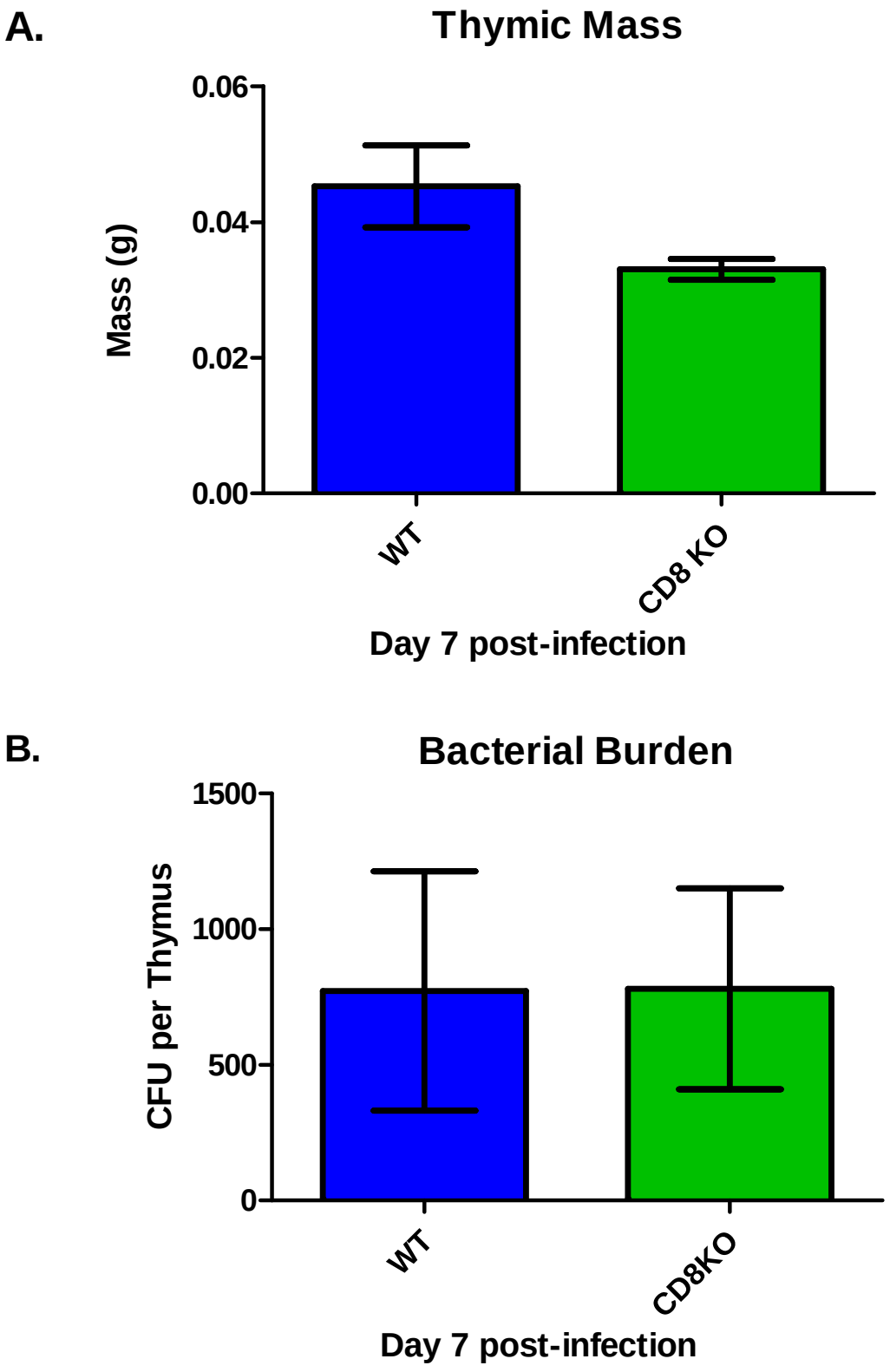

Figure 3.14. At day 7 post-infection, thymic atrophy is observed, but bacterial burden is similar in WT and CD8 KO mice. (A) Thymic atrophy was observed by day 7 post-infection in both WT and CD8 KO mice (B) Bacterial burden of the thymus is similar in WT and CD8 KO mice at day 7 post-infection. Data is taken from one experiment where n=4. The Mann-Whitney U test was used to confirm statistical significance. Data represented as mean ±SEM. * represents statistically significant data ($P<0.05$).

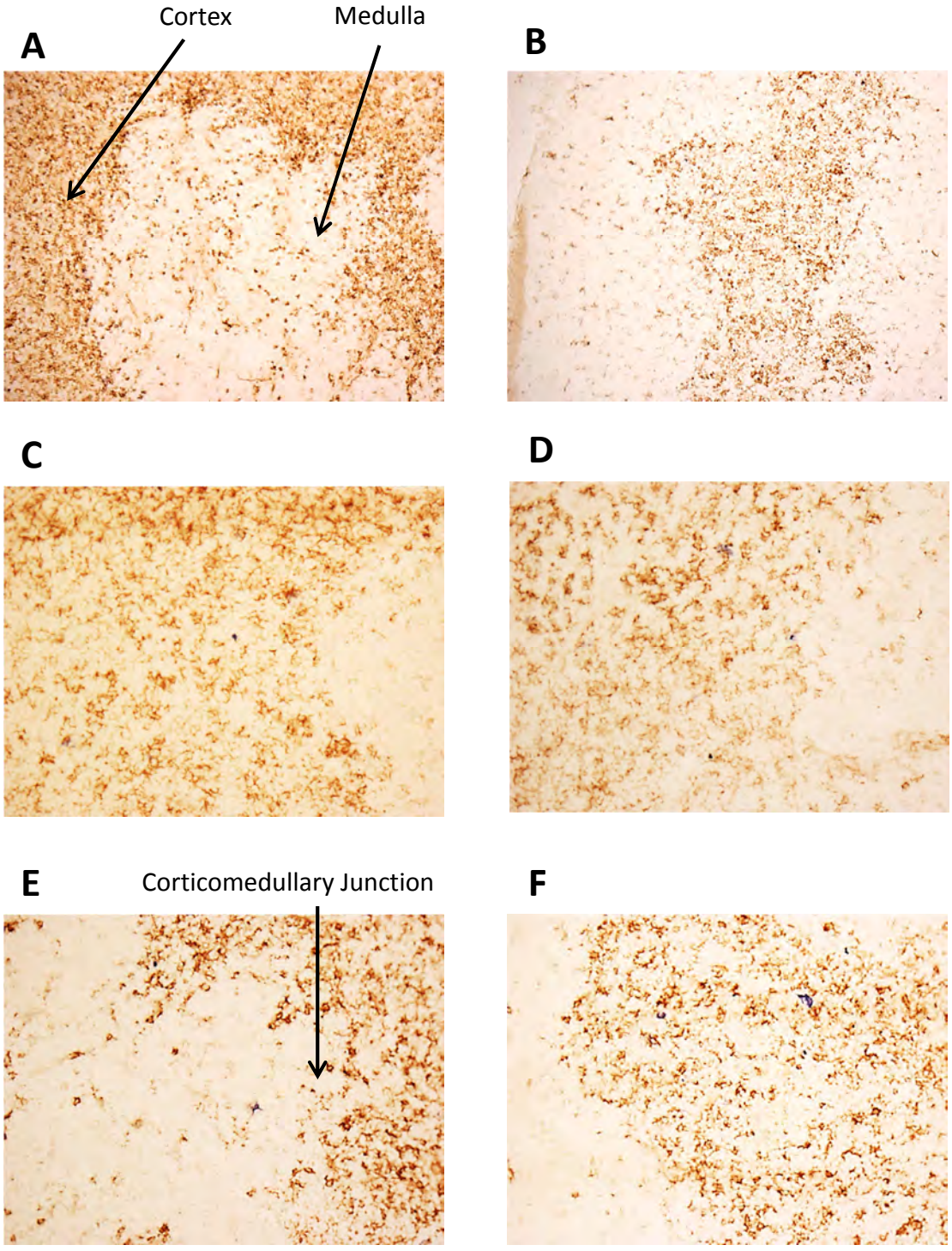

Figure 3.15. IHC staining for F4/80^{+}(blue) and CD11c (brown) thymic macrophages at the corticomedullary junction . Thymus sections were taken from WT and CD8 KO mice, respectively at days 0 (A and B), 7 (C and D), and 35 (E and F) post-infection. (A and B are x10 images) (C-F are x20 images).

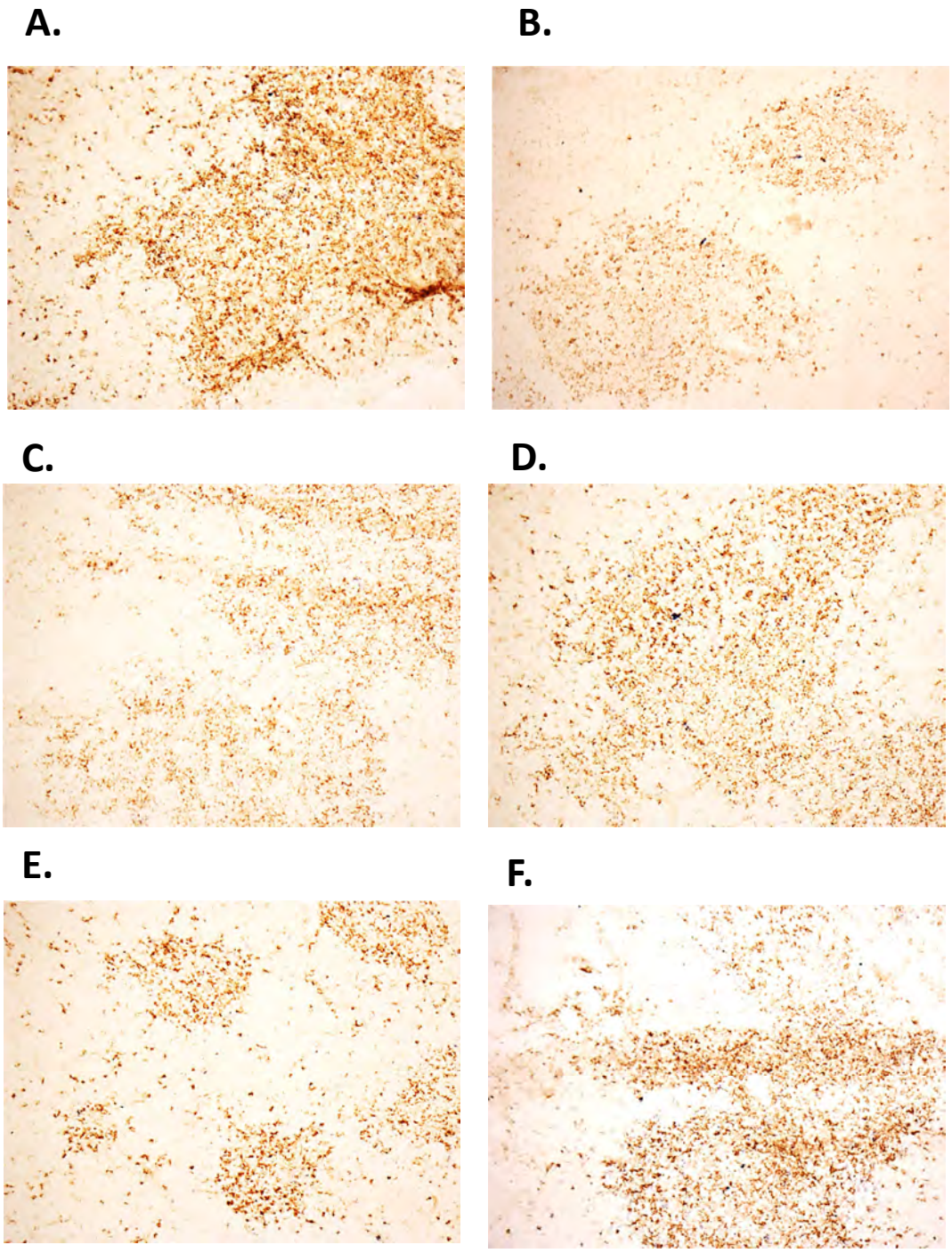

Figure 3.16. IHC staining for B220^{+} (blue) and CD11c^{+} (brown) plasmacytoid DCs (pDCs) (x10 magnification) . Thymus sections were taken from WT and CD8 KO mice, respectively at days 0 (A and B), 7 (C and D), and 35 (E and F) post-infection.

A.

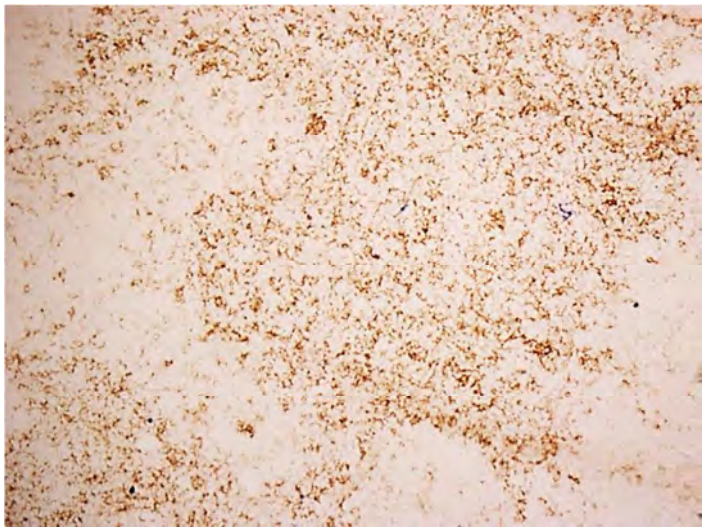

B.

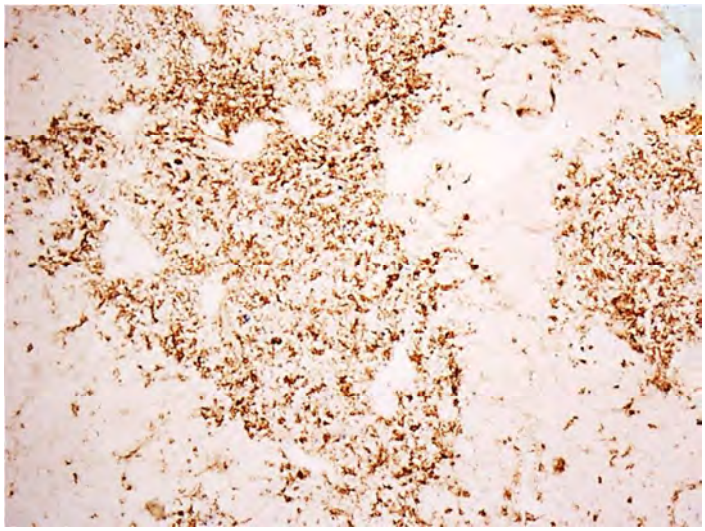

Figure 3.17. IHC staining for CD103 (blue) and CD11c (brown) (x10 magnification) . Thymus sections were taken from WT and CD8 KO mice, respectively at days 7 (A and B) post-infection.

Chapter 4: Discussion

4.1 A role for CD8 in the primary response to STm infection

Prior to this study, it has been evidenced that the lack of CD8 molecules does not impact the MHC Class II restricted helper T-cell response in STm infection (Fung-Leung et al., 1991). Although there were no statistically significant differences within the splenic T-cell populations in WT and CD8KO mice, CD8 KO mice did not effectively clear bacteria as well as WT mice at day 35 post-infection within the spleen. However, this was not reflected in the splenic masses as there was no additional evidence of increased splenomegaly at day 35 within CD8 KO mice. Splenic masses and bacterial burden should decrease by day 35 in both WT and CD8 KO mice during STm infection as evidenced by Jackson et al. (2010). Thus, these experiments would need to be repeated at day 35 in order to determine splenic masses and bacterial loads in CD8 KO mice. This suggests that $CD8^+$T-cells may play a minor role in establishing bacterial clearance during primary infection. Previous studies have shown that CD8-deficient mice that have been challenged with an attenuated strain of STm only show a mild deficiency in effectively clearing STm (Moon and McSorley, 2009).

Also, $CD8^+$T-cells have played a role in bacterial clearance at the latter stages of attenuated STm infection in conjunction with perforin and granzyme B, which are both proteins that provide for the cytolytic nature of $CD8^+$CTLs (Lee et al., 2012). Lee et al. (2012) has hypothesized that $CD8^+$CTLs may play a synergistic role in the primary stages of STm infection with regards to the release and presentation of STm antigens to MHC class-II restricted $CD4^+$T-cells. This hypothesis can be confirmed by the fact that $CD8^+$T-cells respond to T-helper 2 (Th2) presented antigens and induce Th1 cytokines,

which in turn enhances the proliferation and differentiation of B-cells and $CD4^+$T-cells, which are extremely important in mounting an immune response against STm (Mohr et al., 2010).

This may be correlated with the lower levels of OMP-specific IgG antibody titres seen at day 7 post-infection in CD8 KO mice.

IgG is the most abundant antibody present in the immune response against STm (Goh et al., 2011). Previously, it has been shown to confer protection against secondary virulent STm infections in mice (Goh et al., 2011). Furthermore, four subclasses of IgG exist within the murine model and their flexibility is characterised as follows: IgG2b>IgG2a>IgG3>IgG1 (Roux et al., 1997).

IgG, IgG2b, and IgG2a (trend) (IgG2c in C57BL/6 mice (Martin et al., 1998)) antibody responses to OMPs were found to be significantly lower in CD8 KO mice. Please note that WT and CD8 KO mice were immunised with purified porins in preliminary experiments to characterise the antibody-mediated response to STm infection; however, only two mice appeared to be protected once challenged with STm. It was difficult to assess whether or not the porins or STm were administered successfully by i.p. injection. Thus, we decided not to pursue these experiments (data is not shown).

It has been evidenced that T-dependent switching to IgG2b and IgG2a (IgG2c) reflects an early, extrafollicular (EF), Th1-mediated response within the first three weeks of STm infection (Cunningham et al., 2007). They also contribute to memory B-cell responses to STm (Secundino et al., 2006). Furthermore, it was evidenced by Cunningham et al. (2007) that IgG2c antibody responses to OMPs could be detected by day 7 post-infection

in WT mice and that OMPs were major targets of early, switched IgG2c antibody responses. Therefore, the EF response is integral in mediating bacteraemia and can protect against subsequent STm infections (Cunningham et al., 2007).

Clearly, the higher bacterial burdens at day 35 and the lower levels of OMP-specific IgG at day 7 post-infection suggest a defect in the early EF response to STm. Thus, the absence of CD8 molecules must impact the early T_{FH} response during thymus-dependent (TD) antibody responses. T_{FH} cells induce the production of IFN-γ, which is known to mediate bacterial clearance, as well as isotype class switching.

Previously, it has been shown that STm infections induce a strong EF plasma cell response, which produces IgM (TI response) and IgG class-switching of B-cells to IgG2a (IgG2c in C57BL/6 mice) and IgG2b (TD response) (Lee et al., 2011). This is evidenced here in this investigation with regards to WT mice, but is absent in CD8 KO mice.

$CD8^+$T-cells when primed by alum-precipitated proteins have been shown to produce IFN-γ (Mohr et al., 2010). Additionally, STm-specific $CD8^+$T-cells primed with alum-precipitated proteins can contribute to antibody class switching from IgG1 (Th2) to IgG2a (IgG2c in C57BL/6 mice) and IgG2b (Th1). It is unclear how $CD8^+$T-cells affect class-switching in B-cell follicles in the spleen since these cells aren't found there; however, they produce IFN-γ, which leads to the migration of Th1 cells to germinal centres in the spleen (Mohr et al., 2010). Furthermore, Mohr et al. (2010) has shown that ovalbumin-specific $CD8^+$T-cells (OTI) may indirectly induce class-switching from the outer T-zone located in the white pulp of the spleen.

In a recent study, it was found that IgG allows DCs to process and present antigen efficiently to T-cells once challenged with STm (Riquelme et al., 2012). The presence of IgG within immune complexes initiates the phagocytosis of antigens (Riquelme et al., 2012). The mechanism behind this phenomenon could be due to the suppression of the release of SP1-1 (*Salmonella* Pathogenicity Island-1) derived effectors that inhibit DC-mediated phagocytosis of STm (Riquelme et al., 2012). Furthermore, the event of IgG2a (IgG2c) isotype being bound to FcγRI allows for the phagocytosis of pathogens via enhancing the production of reactive oxygen intermediates (Goh et al., 2011).

Lower relative titres of IgG antibody may inhibit bacterial clearance in mice during the primary immune response. This hypothesis is concurrent within the results from this study where CD8 KO mice had higher bacterial burdens in contrast to WT mice at day 35 post-infection. This suggests that the lower levels of IgG at day 7 post-infection inhibit bacterial clearance later on in STm infection, even though IgG titres return to normal levels at day 35 post-infection.

Interestingly, this phenomenon challenges the results from previous studies that suggest that CD8-deficient mice are not inhibited in resolving primary STm infection with an attenuated strain of STm (Ravindran and McSorley, 2005).

However, it has been suggested IgG antibody responses may contribute more to the inhibition of STm-specific responses that inhibit DC priming of naïve T-cells rather than bacterial clearance (Ravindran and McSorley, 2005).

Splenic B-cell transitional WT and CD8 KO populations gated on $B220^{+}$ and IgM^{+} at day 0 were statistically different from one another. The small differences in baseline

transitional B-cell numbers could be due to various reasons, which weren't pursued in this investigation. However, it can be hypothesised that the absence of $CD8^+$T-cells in CD8 KO mice may contribute to their niche being occupied by more transitional B-cells as there isn't an increase in $CD4^+$T-cell numbers seen at day 0.

Please note that PBS controls were included in experiments on Days 7 and 35 post-infection; however, they were not included in experiments on Day 0 in order to avoid unnecessary physiological stress to the mice immediately before they were sacrificed. If the mice were immediately sacrificed after injection, this stress may have been reflected in the results such as the quantification of splenic T and B-cell populations.

DC populations in the thymus were visualised via IHC staining; however, they were not assessed by IHC in the spleen nor flow cytometry (thymus only). There were no detectable differences between $F4/80^+CD11c^+$ thymic macrophages, $B220^+CD11c^+$ plasmacytoid cells, nor $CD103^+CD11c^+$ dendritic cells in WT and CD8 KO mice. In fact, these dendritic cell populations were quite rare in the thymus. Furthermore, the thymic mass and bacterial burden did not differ between WT and CD8 KO mice. Thus, it was difficult to assess the relationship between IgG and DC priming of naïve T-cells.

It has been documented that studies using attenuated strains of STm have lower invasion and intracellular replication rates (Lo et al., 1999). Therefore, these types of infections could induce a weak $CD8^+$CTL response, which is non-reflective of infection with a virulent strain of STm (Lo et al., 1999). Furthermore, other studies have shown that vaccine-induced protection once challenged with virulent strains of STm is significantly reduced (Mittrucker et al., 2002).

More importantly, a study has shown that $CD8^+$T-cell programming for differentiation, proliferation, and contraction is dependent on host-interactions with STm (Luu et al., 2006). Their model evidenced that the presentation of STm antigens to $CD8^+$T-cells occurs within the first few days of infection and peaks at day 7 of the infection (Luu et al., 2006). In fact, different strains of STm may affect the differentiation of $CD8^+$T-cells due to differences in the genetic background of the host, route of infection, infectious dose, degree of host inflammation, growth rate, and intracellular location (Luu et al., 2006, Mastroeni and Sheppard, 2004).

Furthermore, studies have suggested that intravenous (IV) and intraperitoneal (IP) routes of infection, as well as using attenuated strains of STm have led to inconsistent results (Hughes and Galan, 2002).

4.2 Future work

With regards to my immediate future plans, I would increase the sample size and repeat experiments, particularly at day 7 post-infection, in order to achieve a more robust statistical analysis. Furthermore, I would repeat experiments at day 35 in order to investigate the differences in splenic bacterial burden seen between WT and CD8 KO mice. Additionally, if there was still evidence of an increased bacterial load at day 35 in CD8 KO mice and no statistical difference in their splenic masses from day 7 to day 35, then I would carry out and investigate the correlation between the increased bacterial burden and the lack of additional splenomegaly.

I would like to investigate a few areas in the future due to the defect in the early T_{FH} response at day 7and the reduced bacterial clearance at day 35 post-infection in CD8 KO

mice. It would be interesting to challenge CD8 KO mice with a virulent strain of STm, such as SL1344, to see if previous infection with the attenuated strain of STm, SL3261, confers cross-protection via bacterial clearance and/or an antibody-mediated response.

Furthermore, it would be interesting to deliver STm-specific IgG to CD8 KO mice in order to mount an IgG antibody-mediated response at day 7 post-challenge with STm. Furthermore, STm-specific IgG may significantly reduce bacterial titres once challenged with STm at day 35 post-infection in CD8 KO mice.

Additionally, I would employ confocal microscopy and flow cytometry techniques in order to visualize and quantify DC numbers in the thymus as they were very rare and difficult to visualise by IHC.

Acknowledgements

First and foremost, I would like to thank my supervisors, Adam Cunningham and Graham Anderson for their support in this 20-week project. Additionally, I would like to thank the Cunningham research group, which includes: Saeeda Bobat, Jessica Hitchcock, and Adriana Flores-Langarica for their tremendous help with the animal work and lab techniques throughout the entire project. I'd like to thank Charlotte Cook and Sarah Cook for their advice and vast knowledge of the techniques that I have used and acquired during this term. Additionally, I'd like to thank Ewan Ross for his advice on the thymus and its role in STm infection. These individuals are driven, enthusiastic, and hard-working and I've admired them throughout the entire project. I would not have been able to complete this project without their collective support and have enjoyed the entire experience.

Finally, I'd like to thank my family, friends, and partner for their continuous support during this 20-week project. Without their constant belief and confidence in me, I would not have been able to complete this project nor this Master's degree. Thank you for providing a solid foundation that has allowed me to grow within the academic world and more importantly, as an individual that can achieve anything she sets out to complete!

References

BANCHEREAU, J. & STEINMAN, R. M. 1998. Dendritic cells and the control of immunity. *Nature,* 392**,** 245-252.

CROTTY, S. 2011. Follicular helper CD4 T cells (TFH). *Annu Rev Immunol,* 29**,** 621-63.

CUNNINGHAM, A. F., GASPAL, F., SERRE, K., MOHR, E., HENDERSON, I. R., SCOTT-TUCKER, A., KENNY, S. M., KHAN, M., TOELLNER, K. M., LANE, P. J. & MACLENNAN, I. C. 2007. Salmonella induces a switched antibody response without germinal centers that impedes the extracellular spread of infection. *J Immunol,* 178**,** 6200-7.

DEL RIO, M. L., BERNHARDT, G., RODRIGUEZ-BARBOSA, J. I. & FORSTER, R. 2010. Development and functional specialization of CD103+ dendritic cells. *Immunol Rev,* 234**,** 268-81.

DOUGAN, G., JOHN, V., PALMER, S. & MASTROENI, P. 2011. Immunity to salmonellosis. *Immunological reviews,* 240**,** 196-210.

FUNG-LEUNG, W. P., SCHILHAM, M. W., RAHEMTULLA, A., KUNDIG, T. M., VOLLENWEIDER, M., POTTER, J., VAN EWIJK, W. & MAK, T. W. 1991. CD8 is needed for development of cytotoxic T cells but not helper T cells. *Cell,* 65**,** 443-9.

GERMAIN, R. N. 2002. T-cell development and the CD4-CD8 lineage decision. *Nat Rev Immunol,* 2**,** 309-22.

GIL-CRUZ, C., BOBAT, S., MARSHALL, J. L., KINGSLEY, R. A., ROSS, E. A., HENDERSON, I. R., LEYTON, D. L., COUGHLAN, R. E., KHAN, M., JENSEN, K. T., BUCKLEY, C. D., DOUGAN, G., MACLENNAN, I. C., LOPEZ-MACIAS, C. & CUNNINGHAM, A. F. 2009. The porin OmpD from nontyphoidal Salmonella is a key target for a protective B1b cell antibody response. *Proc Natl Acad Sci U S A,* 106**,** 9803-8.

GOG, J. R., MURCIA, A., OSTERMAN, N., RESTIF, O., MCKINLEY, T. J., SHEPPARD, M., ACHOURI, S., WEI, B., MASTROENI, P., WOOD, J. L., MASKELL, D. J., CICUTA, P. & BRYANT, C. E. 2012. Dynamics of Salmonella infection of macrophages at the single cell level. *J R Soc Interface,* 9**,** 2696-707.

GOH, Y. S., GRANT, A. J., RESTIF, O., MCKINLEY, T. J., ARMOUR, K. L., CLARK, M. R. & MASTROENI, P. 2011. Human IgG isotypes and activating Fcgamma receptors in the interaction of Salmonella enterica serovar Typhimurium with phagocytic cells. *Immunology,* 133**,** 74-83.

GRIFFIN, A. J. & MCSORLEY, S. J. 2011. Development of protective immunity to Salmonella, a mucosal pathogen with a systemic agenda. *Mucosal Immunol,* 4**,** 371-82.

HENSEL, M. 2000. Salmonella pathogenicity island 2. *Mol Microbiol,* 36**,** 1015-23.

HESS, J., LADEL, C., MIKO, D. & KAUFMANN, S. H. 1996. Salmonella typhimurium aroA- infection in gene-targeted immunodeficient mice: major role of CD4+ TCR-alpha beta cells and IFN-gamma in bacterial clearance independent of intracellular location. *J Immunol,* 156**,** 3321-6.

HOISETH, S. K. & STOCKER, B. A. 1981. Aromatic-dependent Salmonella typhimurium are non-virulent and effective as live vaccines. *Nature,* 291**,** 238-9.

HUGHES, E. A. & GALAN, J. E. 2002. Immune response to Salmonella: location, location, location? *Immunity,* 16**,** 325-8.

IBARRA, J. A. & STEELE-MORTIMER, O. 2009. Salmonella--the ultimate insider. Salmonella virulence factors that modulate intracellular survival. *Cell Microbiol,* 11**,** 1579-86.

JACKSON, A., NANTON, M. R., O'DONNELL, H., AKUE, A. D. & MCSORLEY, S. J. 2010. Innate immune activation during Salmonella infection initiates extramedullary erythropoiesis and splenomegaly. *J Immunol,* 185**,** 6198-204.

JANEWAY, C., TRAVERS, P., WALPORT, M. & SHLOMCHIK, M. 2005. Immunobiology. 6th. *Garland Science*.

LEE, S. J., DUNMIRE, S. & MCSORLEY, S. J. 2012. MHC class-I-restricted CD8 T cells play a protective role during primary Salmonella infection. *Immunol Lett,* 148**,** 138-43.
LEE, S. K., RIGBY, R. J., ZOTOS, D., TSAI, L. M., KAWAMOTO, S., MARSHALL, J. L., RAMISCAL, R. R., CHAN, T. D., GATTO, D., BRINK, R., YU, D., FAGARASAN, S., TARLINTON, D. M., CUNNINGHAM, A. F. & VINUESA, C. G. 2011. B cell priming for extrafollicular antibody responses requires Bcl-6 expression by T cells. *J Exp Med,* 208**,** 1377-88.
LI, J., PARK, J., FOSS, D. & GOLDSCHNEIDER, I. 2009. Thymus-homing peripheral dendritic cells constitute two of the three major subsets of dendritic cells in the steady-state thymus. *J Exp Med,* 206**,** 607-22.
LO, W. F., ONG, H., METCALF, E. S. & SOLOSKI, M. J. 1999. T cell responses to Gram-negative intracellular bacterial pathogens: a role for CD8+ T cells in immunity to Salmonella infection and the involvement of MHC class Ib molecules. *J Immunol,* 162**,** 5398-406.
LUU, R. A., GURNANI, K., DUDANI, R., KAMMARA, R., VAN FAASSEN, H., SIRARD, J. C., KRISHNAN, L. & SAD, S. 2006. Delayed expansion and contraction of CD8+ T cell response during infection with virulent Salmonella typhimurium. *J Immunol,* 177**,** 1516-25.
MACLENNAN, C. A., GONDWE, E. N., MSEFULA, C. L., KINGSLEY, R. A., THOMSON, N. R., WHITE, S. A., GOODALL, M., PICKARD, D. J., GRAHAM, S. M., DOUGAN, G., HART, C. A., MOLYNEUX, M. E. & DRAYSON, M. T. 2008. The neglected role of antibody in protection against bacteremia caused by nontyphoidal strains of Salmonella in African children. *J Clin Invest,* 118**,** 1553-62.
MACLENNAN, I. C. 1994. Germinal centers. *Annual review of immunology,* 12**,** 117-139.
MACLENNAN, I. C., TOELLNER, K. M., CUNNINGHAM, A. F., SERRE, K., SZE, D. M., ZUNIGA, E., COOK, M. C. & VINUESA, C. G. 2003. Extrafollicular antibody responses. *Immunol Rev,* 194**,** 8-18.
MARSHALL, J. L., FLORES-LANGARICA, A., KINGSLEY, R. A., HITCHCOCK, J. R., ROSS, E. A., LOPEZ-MACIAS, C., LAKEY, J., MARTIN, L. B., TOELLNER, K. M., MACLENNAN, C. A., MACLENNAN, I. C., HENDERSON, I. R., DOUGAN, G. & CUNNINGHAM, A. F. 2012. The capsular polysaccharide Vi from Salmonella typhi is a B1b antigen. *J Immunol,* 189**,** 5527-32.
MARTIN, F. & KEARNEY, J. F. 2002. Marginal-zone B cells. *Nat Rev Immunol,* 2**,** 323-35.
MARTIN, R. M., BRADY, J. L. & LEW, A. M. 1998. The need for IgG2c specific antiserum when isotyping antibodies from C57BL/6 and NOD mice. *J Immunol Methods,* 212**,** 187-92.
MASTROENI, P., GRANT, A., RESTIF, O. & MASKELL, D. 2009. A dynamic view of the spread and intracellular distribution of Salmonella enterica. *Nat Rev Microbiol,* 7**,** 73-80.
MASTROENI, P. & SHEPPARD, M. 2004. Salmonella infections in the mouse model: host resistance factors and in vivo dynamics of bacterial spread and distribution in the tissues. *Microbes Infect,* 6**,** 398-405.
MASTROENI, P., VILLARREAL-RAMOS, B. & HORMAECHE, C. E. 1992. Role of T cells, TNF alpha and IFN gamma in recall of immunity to oral challenge with virulent salmonellae in mice vaccinated with live attenuated aro- Salmonella vaccines. *Microb Pathog,* 13**,** 477-91.
MEBIUS, R. E. & KRAAL, G. 2005. Structure and function of the spleen. *Nat Rev Immunol,* 5**,** 606-16.
MILES, A. A., MISRA, S. S. & IRWIN, J. O. 1938. The estimation of the bactericidal power of the blood. *J Hyg (Lond),* 38**,** 732-49.
MITTRUCKER, H. W. & KAUFMANN, S. H. 2000. Immune response to infection with Salmonella typhimurium in mice. *J Leukoc Biol,* 67**,** 457-63.
MITTRUCKER, H. W., KOHLER, A. & KAUFMANN, S. H. 2002. Characterization of the murine T-lymphocyte response to Salmonella enterica serovar Typhimurium infection. *Infect Immun,* 70**,** 199-203.
MOHR, E., CUNNINGHAM, A. F., TOELLNER, K. M., BOBAT, S., COUGHLAN, R. E., BIRD, R. A., MACLENNAN, I. C. & SERRE, K. 2010. IFN-{gamma} produced by CD8 T cells induces T-bet-dependent and -independent class switching in B cells in responses to alum-precipitated protein vaccine. *Proc Natl Acad Sci U S A,* 107**,** 17292-7.

MOON, J. J. & MCSORLEY, S. J. 2009. Tracking the dynamics of salmonella specific T cell responses. *Curr Top Microbiol Immunol,* 334**,** 179-98.
NAUCIEL, C. 1990. Role of CD4+ T cells and T-independent mechanisms in acquired resistance to Salmonella typhimurium infection. *J Immunol,* 145**,** 1265-9.
NUNES-ALVES, C., NOBREGA, C., BEHAR, S. M. & CORREIA-NEVES, M. 2013. Tolerance has its limits: how the thymus copes with infection. *Trends Immunol*.
O'SHEA, J. J. & PAUL, W. E. 2010. Mechanisms underlying lineage commitment and plasticity of helper CD4+ T cells. *Science,* 327**,** 1098-102.
OKADA, T., LIAN, Z. X., NAIKI, M., ANSARI, A. A., IKEHARA, S. & GERSHWIN, M. E. 2003. Murine thymic plasmacytoid dendritic cells. *European journal of immunology,* 33**,** 1012-1019.
RAVINDRAN, R. & MCSORLEY, S. J. 2005. Tracking the dynamics of T-cell activation in response to Salmonella infection. *Immunology,* 114**,** 450-8.
RIQUELME, S. A., BUENO, S. M. & KALERGIS, A. M. 2012. IgG keeps virulent Salmonella from evading dendritic cell uptake. *Immunology,* 136**,** 291-305.
ROSS, E. A., COUGHLAN, R. E., FLORES-LANGARICA, A., LAX, S., NICHOLSON, J., DESANTI, G. E., MARSHALL, J. L., BOBAT, S., HITCHCOCK, J., WHITE, A., JENKINSON, W. E., KHAN, M., HENDERSON, I. R., LAVERY, G. G., BUCKLEY, C. D., ANDERSON, G. & CUNNINGHAM, A. F. 2012. Thymic function is maintained during Salmonella-induced atrophy and recovery. *J Immunol,* 189**,** 4266-74.
ROUX, K. H., STRELETS, L. & MICHAELSEN, T. E. 1997. Flexibility of human IgG subclasses. *The Journal of Immunology,* 159**,** 3372-82.
SANTOS, R. L., ZHANG, S., TSOLIS, R. M., KINGSLEY, R. A., ADAMS, L. G. & BAUMLER, A. J. 2001. Animal models of Salmonella infections: enteritis versus typhoid fever. *Microbes Infect,* 3**,** 1335-44.
SECUNDINO, I., LOPEZ-MACIAS, C., CERVANTES-BARRAGAN, L., GIL-CRUZ, C., RIOS-SARABIA, N., PASTELIN-PALACIOS, R., VILLASIS-KEEVER, M. A., BECKER, I., PUENTE, J. L., CALVA, E. & ISIBASI, A. 2006. Salmonella porins induce a sustained, lifelong specific bactericidal antibody memory response. *Immunology,* 117**,** 59-70.
SHORTMAN, K. & LIU, Y. J. 2002. Mouse and human dendritic cell subtypes. *Nat Rev Immunol,* 2**,** 151-61.
TZELEPIS, F., ALCON, V., DUDANI, R., GURNANI, K., ZAFER, A., EVERSON, E. S., YOUNG, K. G., RUSSMANN, H., KRISHNAN, L. & SAD, S. 2012. Modulation of antigenic location converts chronic into acute infection by forcing CD8+ T cell recognition. *Cell Rep,* 2**,** 1710-21.
VALE, A. M. & SCHROEDER, H. W., JR. 2010. Clinical consequences of defects in B-cell development. *J Allergy Clin Immunol,* 125**,** 778-87.
VAN DER VELDEN, A. W., COPASS, M. K. & STARNBACH, M. N. 2005. Salmonella inhibit T cell proliferation by a direct, contact-dependent immunosuppressive effect. *Proc Natl Acad Sci U S A,* 102**,** 17769-74.
VOEDISCH, S., KOENECKE, C., DAVID, S., HERBRAND, H., FÖRSTER, R., RHEN, M. & PABST, O. 2009. Mesenteric lymph nodes confine dendritic cell-mediated dissemination of Salmonella enterica serovar Typhimurium and limit systemic disease in mice. *Infection and immunity,* 77**,** 3170-3180.